

FALCON: Honest-Majority Maliciously Secure Framework for Private Deep Learning

Sameer Wagh
Princeton University

Shruti Tople
Microsoft Research

Fabrice Benhamouda
Algorand Foundation

Eyal Kushilevitz
Technion

Prateek Mittal
Princeton University

Tal Rabin
Algorand Foundation

Abstract

This paper aims to enable training and inference of neural networks in a manner that protects the privacy of sensitive data. We propose FALCON – an end-to-end 3-party protocol for fast and secure computation of deep learning algorithms on large networks. FALCON presents three main advantages. It is highly *expressive*. To the best of our knowledge, it is the first secure framework to support high capacity networks with over a hundred million parameters such as VGG16 as well as the first to support batch normalization, a critical component of deep learning that enables training of complex network architectures such as AlexNet. Next, FALCON guarantees *security with abort* against malicious adversaries, assuming an honest majority. It ensures that the protocol always completes with correct output for honest participants or aborts when it detects the presence of a malicious adversary. Lastly, FALCON presents new theoretical insights for protocol design that make it *highly efficient* and allow it to outperform existing secure deep learning solutions. Compared to prior art for private inference, we are about $8\times$ faster than SecureNN (PETS '19) on average and comparable to ABY³ (CCS '18). We are about $16 - 200\times$ more communication efficient than either of these. For private training, we are about $6\times$ faster than SecureNN, $4.4\times$ faster than ABY³ and about $2 - 60\times$ more communication efficient. This is the first paper to show via experiments in the WAN setting, that for multi-party machine learning computations over large networks and datasets, *compute operations* dominate the overall latency, as opposed to the communication.

1 Introduction

With today's digital infrastructure, tremendous amounts of private data is continuously being generated – data which combined with deep learning algorithms can transform the current social and technological landscape. For example, distribution of child exploitative imagery has plagued social media platforms [1, 2]. However, stringent government regulations hamper automated detection of such harmful content.

Support for secure computation of state-of-the-art image classification networks would aid in detecting child exploitative imagery on social media. Similarly, there is promise in analyzing medical data across different hospitals especially for the treatment of rare diseases [3]. In both these scenarios, multiple parties (i.e., social media platforms or hospitals) could co-operate to train efficient models that have high prediction accuracy. However, the sensitive nature of such data demands deep learning frameworks that allow training on data aggregated from multiple entities while ensuring strong privacy and confidentiality guarantees. A synergistic combination of secure computing primitives with deep learning algorithms would enable sensitive applications to benefit from the high prediction accuracies of neural networks.

Secure multi-party computation (MPC) techniques provide a transformative capability to perform secure analytics over such data [4–6]. MPC provides a cryptographically secure framework for computations where the collaborating parties do not reveal their secret data to each other. The parties only learn the output of the computation on the combined data while revealing nothing about the individual secret inputs. Recently, there has been an of research in reducing the performance overhead of MPC protocols, specifically tailored for machine learning [7–12]. However, there has been less or no effort in advancing the research in other dimensions such as expressiveness, scalability to millions of parameters, and stronger security guarantees that are necessary for practical deployment of secure deep learning frameworks. In this work, we present FALCON — an efficient and expressive 3-party deep learning framework that provides support for both training and inference with malicious security guarantees. Table 1 provides a detailed comparison of FALCON with prior work.

Our Contributions. FALCON makes secure deep learning techniques practical through the following contributions:

Malicious Security: FALCON provides strong security guarantees in an honest-majority adversarial setting. This assumption is similar to prior work where majority of the parties (e.g., 2 out of three) behave honestly [8, 13]. FALCON proposes new protocols that are secure against such corruptions and ensure

that either the computation always correctly completes or aborts detecting malicious activity. We achieve this by designing new protocols for the computation of non-linear functions (like ReLU). While MPC protocols are very efficient at computing linear functions, computing non-linear functions like ReLU is much more challenging. We propose solutions both for the malicious security model and provide even more efficient protocols where semi-honest security is sufficient. We formally prove the security of FALCON using the standard simulation paradigm (see Section 4.1). We implement both the semi-honest and malicious protocols in our end-to-end framework. In this manner, FALCON provides a choice to the developers to select between either of the security guarantees depending on the trust assumption among the parties and performance requirements (improved performance for semi-honest protocols).

Improved Protocols: FALCON combines techniques from SecureNN [7] and ABY³ [8] that result in improved protocol efficiency. We improve the theoretical complexity of the central building block – derivative of ReLU – by a factor of 2× through simplified algebra for fixed point arithmetic. We demonstrate our protocols in a smaller ring size, which is possible using an exact yet expensive truncation algorithm. However, this enables the entire framework to use a smaller datatype, thus reducing their communication complexity at least 2×. This reduced communication is critical to the communication improvements of FALCON over prior work. Furthermore, as can be seen in Section 5, these theoretical improvements lead to even larger practical improvements due to the recursive dependence of the complex functionalities on the improved building blocks. Overall, we demonstrate how to achieve maliciously secure protocols for non-linear operations entirely using arithmetic secret sharing and avoiding the use of interconversion protocols (between arithmetic, Boolean and garbled circuits).

Expressiveness: Our focus is to provide simple yet efficient protocols for the fundamental functionalities commonly used in state-of-the-art neural networks. To this end, FALCON is the first work to demonstrate support for `Batch-Normalization` layers in private machine learning. Batch normalization is critical for stable convergence of networks as well as to reduce the parameter tuning required in machine learning. Furthermore, FALCON supports both private training and private inference. This extensive support makes FALCON expressive, thereby supporting evaluation of large networks with hundreds of millions parameters such as VGG16 [14] and AlexNet [15] over datasets such as MNIST [16], CIFAR-10 [17] as well as Tiny ImageNet [18] including in both the LAN and WAN network settings. Most of the prior work assumes training happens in a trusted environment and hence provide support for only inference service [9–11, 19, 20]. However, sensitive data is often inaccessible even during training as described in our motivating application in Section 2. Designing secure protocols for training is more difficult due to the operations involved in

back-propagation which are not required for inference.

End-to-end Implementation and Results. We implement both the semi-honest and malicious variants of FALCON in our end-to-end framework. The codebase is written in C++ in about 12.3k LOC and is built using the communication backend of SecureNN. We experimentally evaluate the performance overhead of FALCON for both private training and inference on multiple networks and datasets. We use 6 diverse networks ranging from simple 3-layer multi-layer perceptrons (MLP) with about 118,000 parameters to large networks with about 16-layers having 138 Million parameters. We trained these networks on MNIST [16], CIFAR-10 [17] and Tiny ImageNet [18] datasets as appropriate based on the network size. We emphasize that FALCON is the first secure ML framework to support training of high capacity networks such as AlexNet and VGG16 on the Tiny ImageNet dataset. We perform extensive evaluation of our framework in both the LAN and WAN setting as well as semi-honest and malicious adversarial setting. For private inference, we are 16× faster than XONN [9], 32× faster than Gazelle [10], 8× faster than SecureNN, and comparable to ABY³ on average. For private training, we are 4.4× faster than ABY³ and 6× faster than SecureNN [7]. Depending on the network, our protocols can provide *upto an order of magnitude* performance improvement over prior art such as SecureNN. With regards to communication overhead, FALCON is upto two orders of magnitude more communication efficient than prior work for both private training and inference. Our results in the WAN setting show that compute operations dominate the overall latency for large networks in FALCON and not the communication rounds. Thus, we claim that FALCON is an optimized 3-PC framework w.r.t. the communication which is often considered as the main bottleneck in multi-party computation protocols.

2 FALCON Overview

In this section, we describe the application setting for FALCON, provide a motivating application, state the threat model, and the design goals of this work.

2.1 A 3-Party Machine Learning Service

We consider the following scenario. There are two types of users, the first own data on which the learning algorithm will be applied, we call them data holders. The second are users who query the system after the learning period, we call these query users. These two sets of users need not be disjoint. We design a machine learning service. This service is provided by 3 parties which we call computing servers. We assume that government regulations or other social deterrents are sufficient enforcers for non-collusion between these computing servers. The service works in two phases: the training phase where the machine learning model of interest is trained on the data

Comparison	Specification	MiniONN [19]	ABY ³ [8]	Chameleon [11]	EzPC [20]	Gazelle [10]	SecureML [6]	SecureNN [7]	XONN [9]	FALCON (This work)	
MPC Set-up	2PC/3PC	2PC	3PC	2PC	2PC	2PC	2PC	3PC	2PC	3PC	
Theoretical Metrics	Private Capability	Private Inference Private Training	● ○	● ●	● ○	● ○	● ○	● ●	● ○	● ●	
	Adversarial Model	Semi-honest Malicious	● ○	● ●	● ○	● ○	● ○	● ●	● ●	● ●	
	Supported Layers	Linear	●	●	●	●	●	●	●	●	●
		Convolution	●	●	●	●	●	●	●	●	●
		Exact ReLU	●	●	●	●	●	●	●	●	●
		Maxpool	●	●	●	●	●	●	●	●	●
Batch-Norm	○	○	○	○	○	○	●	●	●		
Techniques Used	Homomorphic-Enc.	●	○	○	○	●	●	○	○	○	
	Garbled-Circuits	●	●	●	●	●	●	○	●	○	
	Secret Sharing	●	●	●	●	●	●	●	●	●	
Evaluation Metrics	Networking Infrastructure	LAN WAN	● ○	● ●	● ●	● ○	● ●	● ●	● ○	● ●	
	Evaluation Dataset	MNIST	●	●	●	●	●	●	●	●	●
		CIFAR-10	●	○	●	●	●	○	○	●	●
		Tiny ImageNet	○	○	○	○	○	○	○	○	○
	Network Architectures	From [6]	●	●	●	●	●	●	●	●	●
		From [11]	○	●	●	○	●	○	●	●	●
From [19]		●	●	●	●	●	●	●	●	●	
LeNet		○	○	○	○	○	○	○	○	●	
AlexNet	○	○	○	○	○	○	○	○	○	●	
VGG16	○	○	○	○	○	○	○	○	○	●	

Table 1: Comparison of various private deep learning frameworks. ● indicates the framework supports a feature while ○ indicates not supported feature. ● refers to fair comparison not possible as follows: SecureNN provides malicious privacy but not correctness and supports division but not batch norm, XONN supports a simplified batch norm specific to a binary activation layer, ABY³ does not present WAN results for neural networks, Chameleon evaluates over a network similar to AlexNet but using the simpler mean-pooling operations, and due to the high round complexity and communication, SecureML provides an estimate of their WAN evaluation. 2-party protocols are presented here solely for the sake of comprehensive evaluation of the literature.

of the data holders and the inference phase where the trained model can be queried by the query users. The data holders share their data in a replicated secret sharing form between the 3 computing servers. The 3 computing servers utilize the shared data and securely train the network. After these stage query users can submit queries to the system and receive answers based on the newly constructed model held in shared form by the three servers. In this way, the data holders’ input has complete privacy from each of the 3 computing servers. Furthermore, the query is also submitted in shared form and thus is kept secret from the three servers. Below, we describe a concrete motivating application that would benefit from such a 3-party secure machine learning service.

Motivating Application: Detecting Child Exploitative Images. In recent years, the distribution of child exploitative imagery (CEI) has proliferated with the rise of social media platforms – from half a million reported in between 1998-2008 to around 12 million reports in 2017 and 45 million in 2018 [1, 2]. Given the severity of the problem and stringent laws around the handling of such incidents (18 U.S. Code §2251, 2252), it is important to develop solutions that enable efficient detection and handling of such data while complying with stringent privacy regulations. Given the success of machine learning in image classification tasks, it is desirable

to reap the benefits of the vast research literature of machine learning to better tackle the problem of CEI. However, the inability to generate a database of the original images (due to legal regulations) leads to a problem of lack of training data in machine learning. FALCON provides a cryptographically secure framework for this conundrum, where the client data is split into unrecognizable parts among a number of non-colluding entities. In this way, the solution is two-fold, MPC enables the ability to accumulate good quality training data and at the same time can enable machine-learning-as-a-service (MLaaS) for the problem of CEIs. In this manner, MPC can enable an end-to-end solution to automated detection of CEIs in social media with strong privacy to the underlying data.

2.2 Threat Model

Our threat model assumes an honest majority among the three parties in the setting described above. This is a common adversarial setting considered in previous secure multi-party computation approaches [6, 8, 13, 21]. We consider that one of the three parties can be either semi-honest or malicious. A semi-honest adversary passively tries to learn the secret data of the other parties while a malicious adversary can arbitrarily deviate from the protocol. We assume the private keys of each

of the parties are stored securely and not susceptible to leakage. We do not protect against denial of service attacks where parties refuse to cooperate. Here, FALCON simply resorts to aborting the entire computation.

Assumptions & Scope. The 3 parties each have shared point-to-point communication channels and pairwise shared seeds to use AES as a PRNG to generate cryptographically secure common randomness. We note that as the query users receive the answers to the queries in the clear FALCON does not guarantee protecting the privacy of the training data from attacks such as model inversion, membership inference, and attribute inference [22–24]. Defending against these attacks is an orthogonal problem and hence we consider it out-of-scope for this work. We assume that users provide consistent shares and that model poisoning attacks are out of scope.

2.3 Technical Contributions

In this section, we summarize some of the main contributions of this work with a focus on techniques used to achieve our results and improvements.

Hybrid Integration for Malicious Security. FALCON consists of a hybrid integration of ideas from SecureNN and ABY³ along with newer protocol constructions for privacy preserving deep learning. SecureNN, the closest related prior work, does not provide correctness in the presence of malicious adversaries. Furthermore, the use of semi-honest parties in SecureNN makes it a significant challenge to convert those protocols to provide security against malicious corruptions. To this end, we use replicated secret sharing as our building block and use the redundancy to enforce correct behaviour in our protocols [8, 13, 21]. Note that changing from the 2-out-of-2 secret sharing scheme in SecureNN to a 2-out-of-3 replicated secret sharing fundamentally alters some of the building blocks – these protocols are a new contribution of this work. We work in the three-party setting where at most one party can be corrupt. We prove each building block secure in the Universal Composability (UC) framework by proving our protocols are (1) perfectly secure in the stand-alone model, i.e., the distributions are identical and not just statistically close in a model where the protocol is executed only once; and (2) have straight-line black-box simulators, i.e., only assume oracle access to the adversary and do no rewind. Theorem 1.2 from Kushilevitz *et al.* [25] then implies security under general concurrent composition.

Theoretical Improvements to Protocols. FALCON proposes more efficient protocols for common machine learning functionalities while providing stronger security guarantees. We achieve this through a number of theoretical improvements for reducing both the computation as well as the communication. First, in FALCON all parties execute the same protocol in contrast to SecureNN where the protocol is asymmetric. The uniformity of the parties leads to more optimal

resource utilization. Second, the protocol for derivative of ReLU¹ in SecureNN [7] first transforms the inputs using a `Share Convert` subroutine (into secret shares modulo an odd ring) and then invokes a `Compute MSB` subroutine to compute the most significant bit (MSB) which is closely related to the DReLU function. Each of these subroutines have roughly the same overhead. In FALCON, we show an easier technique using new mathematical insights to compute DReLU which reduces the overhead by over 2×. Note that ReLU and DReLU, non-linear activation functions central to deep learning, are typically the expensive operations in MPC. The first two points above lead to strictly improved protocol for these. Third, FALCON uses a smaller ring size while using an exact yet expensive truncation protocol. This trade-off however allows the entire framework to operate on smaller data-types, thus reducing the communication complexity at least 2×. Furthermore, this communication improvement is amplified with the superlinear dependence of the overall communication on the ring size (cf Table 6). This reduced communication is critical to the communication improvements of FALCON over prior work. In other words, we notice strictly larger performance improvements (than the theoretical improvements) in our end-to-end deployments of benchmarked networks presented in Section 5.

Improved Scope of ML Algorithms. Prior works focus on implementing protocols for linear layers and important non-linear operations while we are the first work to propose and implement an end-to-end protocol for batch normalization. Batch-normalization is widely used in practice for speedy training of neural networks and is critical for machine learning for two reasons. First, it speeds up training by allowing higher learning rates and prevents extreme values of activations [26]. This is an important component of the parameter tuning for neural networks as there is limited “seeing and learning” during private training. Second, it reduces overfitting by providing a slight regularization effect and thus improves the stability of training [26]. In other words, private training of neural networks without batch normalization is generally difficult and requires significant pre-training. To truly enable private deep learning, efficient protocols for batch-normalization are required. Implementing batch normalization in MPC is hard for two reasons, first computing the inverse of a number is generally difficult in MPC. Second, most approximate approaches require the inputs to be within a certain range, i.e., there is a trade-off between having an approximate function for inverse of a number over a large range and the complexity of implementing it in MPC. Through our implementation, we enable batch normalization

¹Note that DReLU, when using fixed point encoding over a ring \mathbb{Z}_L is defined as follows:

$$\text{DReLU}(x) = \begin{cases} 0 & \text{if } x > L/2 \\ 1 & \text{Otherwise} \end{cases} \quad (1)$$

that can allow the training of complex network architectures such as AlexNet (about 60 Million parameters).

Comprehensive Evaluation. As shown in Table 1, there are a number of factors involved in comparing different MPC protocols and that none of the prior works provide a holistic solution. We also thoroughly benchmark our proposed system – we evaluate our approach over 6 different network architectures and over 3 standard datasets (MNIST, CIFAR-10, and Tiny ImageNet). We also benchmark our system in both the LAN and WAN setting, for training as well as for inference, and in both the semi-honest and actively secure adversarial models. Finally, we provide a thorough performance comparison against prior state-of-the-art works in the space of privacy preserving machine learning (including 2PC). We believe that such a comparison, across a spectrum of deployment scenarios, is useful for the broader community of MPC practitioners.

Finally, we note that the insights and techniques developed in this work are broadly applicable. For instance, ReLU is essentially a comparison function which can thus enable a number of other applications – private computation of decision trees, privacy-preserving searching and thresholding, and private sorting.

3 Protocol Constructions

We begin by describing the notation used in this paper. We then describe how basic operations are performed over the secret sharing scheme and then move on to describe our protocols in detail.

3.1 Notation

Let P_1, P_2, P_3 be the parties. We use P_{i+1}, P_{i-1} to denote the next and previous party for P_i (with periodic boundary conditions). In other words, next party for P_3 is P_1 and previous party for P_1 is P_3 . We use $\llbracket x \rrbracket^m$ to denote 2-out-of-3 replicated secret sharing (RSS) modulo m for a general modulus m . For any x let $\llbracket x \rrbracket^m = (x_1, x_2, x_3)$ denote the RSS of a secret x modulo m i.e., $x \equiv x_1 + x_2 + x_3 \pmod{m}$, but they are otherwise random. We use the notation $\llbracket x \rrbracket^m$ to mean (x_1, x_2) is held by P_1 , (x_2, x_3) by P_2 , and (x_3, x_1) by P_3 . We denote by $x[i]$ the i^{th} component of a vector x . In this work, we focus on three different moduli $L = 2^\ell$, a small prime p , and 2. In particular, we use $\ell = 5$, $p = 37$. We use fixed-point encoding with 13 bits of precision. In Π_{Mult} over \mathbb{Z}_p , the multiplications are performed using the same procedure with no truncation. ReLU, which compares a value with 0 in this representation corresponds to a comparison with $2^{\ell-1}$.

3.2 Basic Operations

To ease the exposition of the protocols, we first describe how basic operations can be performed over the above secret

sharing scheme. These operations are extensions of Boolean computations from Araki *et al.* [21] to arithmetic shares, similar to ABY³ [8]. However, ABY³ relies on efficient garbled circuits for non-linear function computation which is fundamentally different than the philosophy of this work which relies on simple modular arithmetic. In this manner, we propose a hybrid integration of ideas from SecureNN and ABY³.

Correlated Randomness: Throughout this work, we will need two basic random number generators. Both of these can be efficiently implemented (using local computation) using PRFs. We describe them below:

1. **3-out-of-3 randomness:** Random $\alpha_1, \alpha_2, \alpha_3$ such that $\alpha_1 + \alpha_2 + \alpha_3 \equiv 0 \pmod{L}$ and party P_i holds α_i
2. **2-out-of-3 randomness:** Random $\alpha_1, \alpha_2, \alpha_3$ such that $\alpha_1 + \alpha_2 + \alpha_3 \equiv 0 \pmod{L}$ and party P_i holds (α_i, α_{i+1}) .

Given pairwise shared random keys k_i (shared between parties P_i and P_{i+1}), the above two can be computed as $\alpha_i = F_{k_i}(\text{cnt}) - F_{k_{i-1}}(\text{cnt})$ and $(\alpha_i, \alpha_{i-1}) = (F_{k_i}(\text{cnt}), F_{k_{i-1}}(\text{cnt}))$ where cnt is a counter incremented after each invocation. This is more formally described later on in Π_{Prep} in Fig. 1.

Linear operations: Let a, b, c be public constants and $\llbracket x \rrbracket^m$ and $\llbracket y \rrbracket^m$ be secret shared. Then $\llbracket ax + by + c \rrbracket^m$ can be locally computed as $(ax_1 + by_1 + c, ax_2 + by_2, ax_3 + by_3)$ and hence are simply local computations.

Multiplications Π_{Mult} : To multiply two shared values together $\llbracket x \rrbracket^m = (x_1, x_2, x_3)$ and $\llbracket y \rrbracket^m = (y_1, y_2, y_3)$, parties locally compute $z_1 = x_1y_1 + x_2y_1 + x_1y_2, z_2 = x_2y_2 + x_3y_2 + x_2y_3$ and $z_3 = x_3y_3 + x_1y_3 + x_3y_1$. At the end of this, z_1, z_2 and z_3 form a 3-out-of-3 secret sharing of $\llbracket z = x \cdot y \rrbracket^m$. Parties then perform *resharing* where 3-out-of-3 randomness is used to generate 2-out-of-3 sharing by sending $\alpha_i + z_i$ to party $i - 1$.

Convolutions and Matrix Multiplications: We rely on prior work to perform convolutions and matrix multiplications over secret shares. To perform matrix multiplications, we note that Π_{Mult} described above extends to incorporate matrix multiplications. To perform convolutions, we simply expand the convolutions into matrix multiplications of larger dimensions (cf Section 5.1 of [7]) and invoke the protocol for matrix multiplications. Note that with fixed point arithmetic, each multiplication protocol has to be followed by the truncation protocol (cf Fig. 1) to ensure correct fixed point precision. For more details on fixed-point multiplication, semi-honest, and malicious variants of this refer to [8, 21].

Reconstruction of $\llbracket x \rrbracket^m$: In the semi-honest setting, each party sends one ring element to the next party, i.e., P_i sends share x_i to P_{i+1} . In the malicious setting, each party sends x_i to P_{i+1} and x_{i+1} to P_{i-1} and aborts if the two received values do not agree. Note that in either case, a single round of communication is required.

Select Shares Π_{SS} : We define a sub-routine Π_{SS} , which will be used a number of times in the descriptions of other functionalities. It takes as input shares of two random values $\llbracket x \rrbracket^L, \llbracket y \rrbracket^L$, and shares of a random bit $\llbracket b \rrbracket^2$. The output $\llbracket z \rrbracket^L$ is

either $\llbracket x \rrbracket^L$ or $\llbracket y \rrbracket^L$ depending on whether $b = 0$ or $b = 1$. To do this, we assume access to shares of a random bit $\llbracket c \rrbracket^2$ and $\llbracket c \rrbracket^L$ (pre-computation). Then we open the bit $(b \oplus c) = e$. If $e = 1$, we set $\llbracket d \rrbracket^L = \llbracket 1 - c \rrbracket^L$ otherwise set $\llbracket d \rrbracket^L = \llbracket c \rrbracket^L$. Finally, we compute $\llbracket z \rrbracket^L = \llbracket (y - x) \cdot d \rrbracket^L + \llbracket x \rrbracket^L$ where $\llbracket (y - x) \cdot d \rrbracket^L$ can be computed using $\Pi_{\text{Mult}}(y - x, d)$.

XOR with public bit b : Given shares of a bit $\llbracket x \rrbracket^m$ and a public bit b , we can locally compute shares of bit $\llbracket y \rrbracket^m = \llbracket x \oplus b \rrbracket^m$ by noting that $y = x + b - 2b \cdot x$. Since b is public, this is a linear operation and can be computed in both the semi-honest and malicious adversary models.

Evaluating $\llbracket (-1)^\beta \cdot x \rrbracket^m$ from $\llbracket x \rrbracket^m$ and $\llbracket \beta \rrbracket^m$: We assume that $\beta \in \{0, 1\}$. We first compute $1 - 2\beta$ and then perform the multiplication protocol described above to obtain $\llbracket (1 - 2\beta)x \rrbracket^m = \llbracket (-1)^\beta \cdot x \rrbracket^m$. We split our computations into data dependent online computations and data independent offline computations. Protocols for offline computations are in Fig. 1.

3.3 Private Compare

This function evaluates the bit $x > r$ where r is public and the parties hold shares of bits of x in \mathbb{Z}_p . Algorithm 1 shows implementation of private compare function.

(A) Step 2: $u[i]$ can be computed by first evaluating shares of $2\beta - 1$ and then computing the product of $(2\beta - 1)$ and $x[i] - r[i]$. This can be done in a single round using one invocation of Π_{Mult} .

(B) Steps 3,4: These are simply local computations. For instance, $\llbracket w[i] \rrbracket = (w[i]_1, w[i]_2, w[i]_3)$ can be computed as $w[i]_j = x[i]_j + \delta_{j1}r[i] - 2r[i]x[i]_j$ where $j \in \{1, 2, 3\}$ and δ_{ij} is the Kronecker delta function and is defined as

$$\delta_{ij} = \begin{cases} 0 & \text{if } i \neq j \\ 1 & \text{if } i = j \end{cases}$$

(C) Step 6 can be computed in $\log_2 \ell + 1^2$ rounds using sequential invocations of the Π_{Mult} with smaller strings.

(D) Steps 7,8: These are once again local computations.

This protocol is an example of the challenges of integrating approaches based on simple modular arithmetic with malicious security. Both SecureNN and FALCON aim to find if there exists an index i such that $c_i = 0$. However, the existence of a semi-honest third party makes checking this much easier in SecureNN. The two primary parties simply blind and mask their inputs and send them to the third party. This is not possible in FALCON due to the stronger adversarial model and requires newer protocol constructions. In particular, we need to multiply all the c_i 's together along with a mask in \mathbb{Z}_p^* and reveal this final product to compute the answer.

²One additional round because of multiplication by random blinding factor.

Algorithm 1 Private Compare $\Pi_{\text{PC}}(P_1, P_2, P_3)$:

Input: P_1, P_2, P_3 hold replicated secret sharing of bits of x in \mathbb{Z}_p .

Output: All parties get shares of the bit $(x > r) \in \mathbb{Z}_2$.

Common Randomness: P_1, P_2, P_3 hold a public ℓ bit integer r , shares of a random bit in two rings $\llbracket \beta \rrbracket^2$ and $\llbracket \beta \rrbracket^p$ and shares of a random/secret integer $m \in \mathbb{Z}_p^*$.

```

1: for  $i = \{\ell, \ell - 1, \dots, 1\}$  do
2:   Compute shares of  $u[i] = (-1)^\beta (x[i] - r[i])$ 
3:   Compute shares of  $w[i] = x[i] \oplus r[i]$ 
4:   Compute shares of  $c[i] = u[i] + 1 + \sum_{k=i+1}^\ell w[k]$ 
5: end for
6: Compute and reveal  $d$  given by  $d := m \cdot \prod_{i=1}^\ell c_i \pmod{p}$ 
7: Let  $\beta' = 1$  if  $(d = 0)$  and 0 otherwise.
8: return Shares of  $\beta' \oplus \beta \in \mathbb{Z}_2$ 

```

3.4 Wrap Function

Central to the computation of operations such as ReLU and DReLU is a comparison function. The wrap functions, wrap_2 and wrap_3 are defined below as a function of the secret shares of the parties and effectively compute the ‘‘carry bit’’ when the shares are added together as integers. Eq. 10 shows that DReLU can be easily computed using the wrap_3 function. So all we require is a secure protocol for wrap_3 . Note that we define two similar functions called ‘‘wrap’’ (denoted by wrap_2 and wrap_3). One function takes three inputs and the other one takes four inputs and are formally defined as follows:

$$\text{wrap}_2(a_1, a_2, L) = \begin{cases} 0 & \text{if } a_1 + a_2 < L \\ 1 & \text{Otherwise} \end{cases} \quad (2)$$

$$\text{wrap}_{3e}(a_1, a_2, a_3, L) = \begin{cases} 0 & \text{if } a_1 + a_2 + a_3 < L \\ 1 & \text{if } L \leq a_1 + a_2 + a_3 < 2L \\ 2 & \text{if } 2L \leq a_1 + a_2 + a_3 < 3L \end{cases} \quad (3)$$

In the rest of the paper, we use the $(\text{mod } 2)$ reduction of the wrap function in Equation 4. We call Eq. 3 the *exact wrap* function and Eq. 4 as simply the wrap function.

$$\text{wrap}_3(a_1, a_2, a_3, L) = \text{wrap}_{3e}(a_1, a_2, a_3, L) \pmod{2} \quad (4)$$

Next we briefly describe the connection between wrap_3 computed on shares a_1, a_2, a_3 and the most significant bit (MSB) of the underlying secret a . Note that $a = a_1 + a_2 + a_3 \pmod{L}$ as a_i 's are shares of a modulo L . Considering this sum as a logic circuit (for instance as a ripple carry adder), we can see that $\text{MSB}(a) = \text{MSB}(a_1) + \text{MSB}(a_2) + \text{MSB}(a_3) + c \pmod{2}$ where c is the carry bit from the previous index. The key insight here is that the carry c from the previous index is simply the wrap_3 function computed on a_i 's (ignoring their MSB's) modulo $L/2$ (this is evident from Eq. 3). And this last operation is synonymous with computing the wrap_3 function on $2a_i$'s modulo L . We will further describe the consequences of this connection in Section 3.5 where we describe a protocol to compute the ReLU and DReLU functions.

Algorithm 2 $\text{wrap}_3 \Pi_{\text{WA}}(P_1, P_2, P_3)$:

Input: P_1, P_2, P_3 hold shares of a in \mathbb{Z}_L .
Output: P_1, P_2, P_3 get shares of a bit $\theta = \text{wrap}_3(a_1, a_2, a_3, L)$
Common Randomness: P_1, P_2, P_3 hold shares $\llbracket r \rrbracket^L$ (random number), $\llbracket r[i] \rrbracket^p$ (shares of bits of r) and $\llbracket \alpha \rrbracket^2$ where $\alpha = \text{wrap}_3(r_1, r_2, r_3, L)$.

- 1: Compute $x_j \equiv a_j + r_j \pmod{L}$ and $\beta_j = \text{wrap}_2(a_j, r_j, L)$
- 2: Reconstruct $x \equiv \sum x_j \pmod{L}$
- 3: Compute $\delta = \text{wrap}_3(x_1, x_2, x_3, L)$ ▷ In the clear
- 4: Run Π_{PC} on x, r to get $\eta = (r > x)$.
- 5: **return** $\theta = \beta_1 + \beta_2 + \beta_3 + \delta - \eta - \alpha$

Algorithm 2 gives the protocol for securely computing the wrap_3 function. Note that wrap_2 function is always computed locally and hence a secure algorithm is not needed for the same. In reference to Algorithm 2, we can write the following sets of equations

$$x = a + r - \eta \cdot L \quad (5)$$

$$x = x_1 + x_2 + x_3 - \delta_e \cdot L \quad (6)$$

$$x_i = a_i + r_i - \beta_i \cdot L \quad \forall i \in \{1, 2, 3\} \quad (7)$$

$$r = r_1 + r_2 + r_3 - \alpha_e \cdot L \quad (8)$$

where δ_e, α_e denote the exact wrap functions. Eq. 6,8 follow from the definition of the exact wrap function, while Eq 5,7 follow from the definition of wrap_2 . Assuming θ_e is the exact wrap function on a_1, a_2, a_3 , Eq. 5-8 together give a constraint

$$\theta_e = \beta_1 + \beta_2 + \beta_3 + \delta_e - \eta - \alpha_e \quad (9)$$

Taking mod 2 reduction of Eq. 9 gives us $\theta = \beta_1 + \beta_2 + \beta_3 + \delta - \eta - \alpha$ which is used to compute wrap_3 as in Algorithm 2.

3.5 ReLU and Derivative of ReLU

We now describe how to construct a protocol for securely computing $\text{ReLU}(a)$ and $\text{DReLU}(a)$ for a given secret a . Recall that we use fixed point arithmetic over \mathbb{Z}_{2^ℓ} for efficiency reasons. Using the natural encoding of native C++ data-types, we know that positive numbers are the first $2^{\ell-1}$ and have their most significant bit equal to 0. Negative numbers, on the other hand are the last $2^{\ell-1}$ numbers in the ℓ -bit range and have their most significant bit equal to 1. Thus, the DReLU function defined by Eq. 1, has a simple connection with the most significant bit (MSB) of the fixed point representation viz., $\text{DReLU}(a) = 1 - \text{MSB}(a)$. Furthermore, in Section 3.4, we have seen the connection between $\text{MSB}(a)$ and wrap_3 . Together, these insights can be distilled into the following equation:

$$\begin{aligned} \text{DReLU}(a) = & \text{MSB}(a_1) \oplus \text{MSB}(a_2) \oplus \text{MSB}(a_3) \\ & \oplus \text{wrap}_3(2a_1, 2a_2, 2a_3, L) \oplus 1 \end{aligned} \quad (10)$$

In particular, Derivative of ReLU can be computed by combining the output of the wrap function with local computations. Finally, for computing ReLU from DReLU , we simply call

Algorithm 3 $\text{ReLU}, \Pi_{\text{ReLU}}(P_1, P_2, P_3)$:

Input: P_1, P_2, P_3 hold shares of a in \mathbb{Z}_L .
Output: P_1, P_2, P_3 get shares of $\text{ReLU}(a)$.
Common Randomness: $\llbracket c \rrbracket^2$ and $\llbracket c \rrbracket^L$ (shares of a random bit in two rings)

- 1: Run Π_{WA} to get $\text{wrap}_3(2a_1, 2a_2, 2a_3, L)$
- 2: Compute $\llbracket b \rrbracket^2$ where $b = \text{DReLU}(a)$ ▷ Local comp. (Eq. 10)
- 3: **return** Output of Π_{SS} run on $\{a, 0\}$ with b as selection.

Π_{SS} (which effectively performs Π_{Mult} on shares of a and shares of $\text{DReLU}(a)$). With these observations, we can implement the ReLU and Derivative of ReLU protocols (see Algorithm 3). Note that the approach here is crucially different from the approach SecureNN uses due to use of fundamentally different building blocks as well as deeper mathematical insights such as Eq. 10. To achieve the DReLU functionality, SecureNN first uses a subroutine to transform the shares of the secret into an odd modulus ring and then uses another subroutine to compute the MSB (cf Section 2.3). Both these subroutines have similar complexities. FALCON on the other hand uses the insight presented in Eq. 10 to completely eliminate the need for these subroutines, improving the efficiency by about $2\times$ and simplifying the overall protocol. This also drastically improves the end-to-end performance (by over $6.4\times$) as the ReLU and DReLU functionalities are the building blocks of every comparison in the network.

3.6 Maxpool and Derivative of Maxpool

The functionality of maxpool simply takes as input a vector of secret shared values and outputs the maximum value. For derivative of maxpool, we need a one-hot vector of the same size as the input where the 1 is at the location of the index of the maximum value. Maxpool can be implemented using a binary sort on the vector of inputs and small amounts of bookkeeping, where the comparisons can be performed using ReLUs. Derivative of maxpool can be efficiently implemented along with maxpool. Algorithm 4 describes these in detail.

Algorithm 4 Maxpool, $\Pi_{\text{Maxpool}}(P_1, P_2, P_3)$:

Input: P_1, P_2, P_3 hold shares of a_1, a_2, \dots, a_n in \mathbb{Z}_L .
Output: P_1, P_2, P_3 get shares of a_k and e_k where $k = \text{argmax}\{a_1, \dots, a_n\}$ and where $e_k = \{e_1, e_2, \dots, e_n\}$ with $e_i = 0 \forall i \neq k$ and $e_k = 1$.
Common Randomness: No additional common randomness required.

- 1: Set $\text{max} \leftarrow a_1$ and $\text{ind} \leftarrow e_1 = \{1, 0, \dots, 0\}$
- 2: **for** $i = \{2, 3, \dots, n\}$ **do**
- 3: Set $d_{\text{max}} \leftarrow (\text{max} - a_i)$ and $d_{\text{ind}} \leftarrow (\text{ind} - e_i)$
- 4: $b \leftarrow \Pi_{\text{DReLU}}(d_{\text{max}})$ ▷ $b \rightarrow$ Derivative of ReLU
- 5: Set max as Π_{SS} output on inputs $\{a_i, \text{max}\}$ using selection b .
- 6: Set ind as Π_{SS} output on inputs $\{e_i, \text{ind}\}$ using selection b .
- 7: **end for**
- 8: **return** max, ind

Algorithm 5 Power, $\Pi_{\text{Pow}}(P_1, P_2, P_3)$:

Input: P_1, P_2, P_3 hold shares of b in \mathbb{Z}_L .
Output: P_1, P_2, P_3 get α in the clear, where $2^{\alpha-1} < b \leq 2^\alpha$.
Common Randomness: No additional common randomness required.

- 1: Set $x \leftarrow b$ and $\alpha \leftarrow 0$
- 2: **for** $i = \{\ell - 1, \dots, 2, 1\}$ **do**
- 3: Set $d_x \leftarrow (x - 2^{2^i + \alpha})$
- 4: $c \leftarrow \Pi_{\text{DRReLU}}(d_x)$ and reconstruct c
- 5: **if** $c = 1$ **then**
- 6: Set $x \leftarrow d_x$ and $\alpha \leftarrow \alpha + 2^i$
- 7: **end if**
- 8: **end for**
- 9: **return** α

3.7 Division and Batch Normalization

Truncation allows parties to securely eliminate lower bits of a secret shared value (i.e., truncation by k bits of a secret $a \rightarrow a/2^k$). However, the problem of dividing by a secret shared number is considerably harder and efficient algorithms rely on either (1) sequential comparison (2) numerical methods. In this work, we use the numerical methods approach for its efficiency. We use the specific choices of initializations given in [27, 28] to efficiently compute division over secret shares. A crucial component of numerical methods is the need to estimate the value of the secret within a range. We achieve this using Algorithm 5. Note that Algorithm 5 outputs the bounding power of 2, which is also what is guaranteed by the functionality. In this way, we only reveal the bounding power of 2 and nothing else.

Algorithm 6 is used to compute the value of a/b where a, b are secret shared. The first step for the algorithm is to transform $b \rightarrow x$ where $x \in [0.5, 1)$. Note that if b has fixed point precision of f_p , then x has to be interpreted as a value with fixed-point precision $f_p + \alpha$ where $2^{\alpha-1} < b \leq 2^\alpha$. Thus we first need to extract α (the appropriate range) using Algorithm 5. Let $w_0 = 2.9142 - 2x$, $\epsilon_0 = 1 - x \cdot w_0$ (cf. [27, 28] for choice of constants). Then an initial approximation for $1/x$ is $w_0 \cdot (1 + \epsilon_0)$. For higher order approximations, set $\epsilon_i = \epsilon_{i-1}^2$ and multiply the previous approximate result by $(1 + \epsilon_i)$ to get a better approximate result. Each successive iteration increases the round complexity by 2. For our value of fixed-point precision, we use the following approximation which works with high accuracy (refer to Section 5 for details):

$$\text{AppDiv}(x) = w_0 \cdot (1 + \epsilon_0)(1 + \epsilon_1)(1 + \epsilon_2) \approx \frac{1}{x} \quad (11)$$

Batch-norm is another important component of neural network architectures. They improve the convergence as well as help automate the training process. Algorithm 7 describes the protocol to compute batch-norm. For step 3, required by Eq. 17c in Appendix, we use Newton's method. We use $2^{-\lceil \alpha/2 \rceil}$ as an initial approximation of $1/\sqrt{\sigma^2 + \epsilon}$, where $2^{\alpha-1} < \sigma^2 + \epsilon \leq 2^\alpha$ and use the successive iterative formula:

$$x_{n+1} = \frac{x_n}{2} (3 - ax_n^2) \quad (12)$$

Algorithm 6 Division, $\Pi_{\text{Div}}(P_1, P_2, P_3)$:

Input: P_1, P_2, P_3 hold shares of a, b in \mathbb{Z}_L .
Output: P_1, P_2, P_3 get shares of a/b in \mathbb{Z}_L computed as integer division with a given fixed precision f_p .
Common Randomness: No additional common randomness required.

- 1: Run Π_{Pow} on b to get α such that $2^{\alpha-1} < b \leq 2^\alpha$
- 2: Compute $w_0 \leftarrow 2.9142 - 2b$
- 3: Compute $\epsilon_0 \leftarrow 1 - b \cdot w_0$ and $\epsilon_1 \leftarrow \epsilon_0^2$ and $\epsilon_2 \leftarrow \epsilon_1^2$
- 4: **return** $aw_0(1 + \epsilon_0)(1 + \epsilon_1)(1 + \epsilon_2)$

Algorithm 7 Batch Norm, $\Pi_{\text{BN}}(P_1, P_2, P_3)$:

Input: P_1, P_2, P_3 hold shares of a_1, a_2, \dots, a_m in \mathbb{Z}_L where m is the size of each batch and shares of two learnable parameters γ, β .
Output: P_1, P_2, P_3 get shares of $\gamma z_i + \beta$ for $i \in [m]$ and $z_i = (a_i - \mu)/(\sqrt{\sigma^2 + \epsilon})$ where $\mu = 1/m \sum a_i$, $\sigma^2 = 1/m \sum (a_i - \mu)^2$, and ϵ is a set constant.
Common Randomness: No additional common randomness required.

- 1: Set $\mu \leftarrow 1/m \cdot \sum a_i$
- 2: Compute $\sigma^2 \leftarrow 1/m \cdot \sum (a_i - \mu)^2$ and let $b = \sigma^2 + \epsilon$
- 3: Run Π_{Pow} on b to find α such that $2^{\alpha-1} < b \leq 2^\alpha$
- 4: Set $x_0 \leftarrow 2^{-\lceil \alpha/2 \rceil}$
- 5: **for** $i \in 0, \dots, 3$ **do**
- 6: Set $x_{i+1} \leftarrow \frac{x_i}{2} (3 - bx_i^2)$
- 7: **end for**
- 8: **return** $\gamma \cdot x_{\text{rnds}} \cdot (a_i - \mu) + \beta$ for $i \in [m]$

Given the strategic choice of initial guess, the number of rounds required for close approximation for our choice of fixed-point precision is 4. However, batch normalization during training is computed by sequentially computing $\sqrt{\sigma^2 + \epsilon}$ and then computing the inverse. This approach is used to optimize the computation required during back-propagation which requires the values of $\sqrt{\sigma^2 + \epsilon}$. For computing the square root of a value a , we use Newton's method given by Eq. 13. This can then be used in conjunction with the inverse computation given by Eq. 11 to complete the batch-norm computations.

$$x_{n+1} = \frac{1}{2} \left(x_n + \frac{a}{x_n} \right) \quad (13)$$

4 Theoretical Analysis

We provide a detailed theoretical analysis of our framework and protocols. In particular, we provide proofs of security and analyze the theoretical complexity.

4.1 Security Proofs

We model and prove the security of our construction in the real world-ideal world simulation paradigm [29–31]. In the real interaction, the parties execute the protocol in the presence of an adversary and the environment. On the other hand, in the ideal interaction, the parties send their inputs to a trusted party that computes the functionality truthfully. Finally, to prove the security of our protocols, for every adversary in the

real interaction, there exists a simulator in the ideal interaction such that the environment cannot distinguish between the two scenarios. In other words, whatever information the adversary extracts in the real interaction, the simulator can extract it in the ideal world as well.

We show that our protocols are perfectly secure (i.e., the joint distributions of the inputs, outputs, and the communication transcripts are exactly the same and not statistically close) in the stand-alone model (i.e., protocol is executed only once), and that they have a straight-line black-box simulators (i.e., only assume oracle access to the adversary and hence do no rewind)³. We then rely on the result of Kushilevitz *et al.* [25] to prove that our protocols are secure under concurrent general composition (Theorem 1.2 in [25]).

Due to space constraints, we formally describe the functionalities in Appendix E. We describe simulators for Π_{PC} (Fig. 9), Π_{WA} (Fig. 10), Π_{ReLU} (Fig. 11), $\Pi_{Maxpool}$ (Fig. 12), Π_{Pow} (Fig. 13), Π_{Div} (Fig. 14), and Π_{BN} (Fig. 15) that achieve indistinguishability. \mathcal{F}_{Mult} , \mathcal{F}_{Trunc} , $\mathcal{F}_{Reconst}$ are identical to prior works [8, 13]. We prove security using the standard indistinguishability argument. To prove the security of a particular functionality, we set-up hybrid interactions where the sub-protocols used in that protocol are replaced by their corresponding ideal functionalities and then prove that the interactions can be simulated. This hybrid argument in effect sets up a series of interactions I_0, I_1, \dots, I_k for some k where I_0 corresponds to the real interaction and I_k corresponds to the ideal interaction. Each neighboring interaction, i.e., I_i, I_{i+1} for $i \in \{0, \dots, k-1\}$ is then shown indistinguishable from each other, in effect showing that the real and ideal interactions are indistinguishable. Without loss of generality, we assume that party P_2 is corrupt. In the *real world*, the adversary \mathcal{A} interacts with the honest parties P_0 and P_1 . In the *ideal world*, the simulator interacts with the adversary and simulates exact transcripts for interactions between the adversary \mathcal{A} and P_0, P_1 . On the other hand, the simulator should be able to extract the adversaries inputs. These inputs are fed to the functionality to generate correct output distributions. Theorems 1-6 gives the indistinguishability of these two interactions.

Theorem 1. Π_{PC} securely realizes \mathcal{F}_{PC} with abort, in the presence of one malicious party in the $(\mathcal{F}_{Mult}, \mathcal{F}_{Reconst}, \mathcal{F}_{Prep})$ -hybrid model.

Proof. We first set up some detail on the proof strategy that is essential for other proofs as well. For the ease of exposition, we describe it in the context of Π_{PC} . The goal of designing a simulator is to be able to demonstrate the ability to produce transcripts that are indistinguishable from the transcripts in the real world. The joint distribution of the inputs and outputs is a part of these transcripts and hence has to be indistinguishable in the two interactions. However, since the honest parties simply forward their inputs to the functionality, the simulator

must be able to extract the inputs of the malicious parties to be able to generate the correct shares for the honest parties.

The usual technique to achieve this is to have the simulator run a simulated version of the protocol internally, i.e., emulating the roles of the honest parties and interacting with the adversary. This is what we call an *internal run*. This internal run can then be used to extract the inputs of the adversarial party (which can then be forwarded to the functionality in the ideal interaction). Note that in the hybrid argument, since the subroutines used in the protocol can be replaced by their corresponding ideal interactions, the simulator can emulate the roles of these trusted functionalities in its internal run.

In the specific context of Π_{PC} , the simulator \mathcal{S} for adversary \mathcal{A} works by playing the role of the trusted party for \mathcal{F}_{Mult} , $\mathcal{F}_{Reconst}$ and \mathcal{F}_{Prep} . To be able to simulate, we need to show that:

1. All the transcripts from the real interactions can be simulated
2. The honest parties receive their outputs correctly.

Simulation follows easily from the protocol and the hybrid argument. The simulator for Π_{Mult} (along with the simulator for $\Pi_{Reconst}$) can be used to simulate the transcripts from Steps 2, 6 (from Algorithm 1). Note that the distributions of these transcripts are all uniformly random values and hence achieve perfect security. Steps 3, 4, 7, and 8 on the other hand are all local and do not need simulation.

To extract the inputs of the malicious party, the simulator uses the fact that it has access to r and β (though \mathcal{F}_{Prep}) and all the internal values for the honest parties (in the internal run) and hence can extract the shares of $x[i]$ from the corrupt party P_2 . Finally, if the protocol aborts at any time in the internal run, then the simulator sends Abort to \mathcal{F}_{PC} otherwise, it inputs the extracted shares of $x[i]$ to \mathcal{F}_{PC} and the honest parties receive their outputs. \square

Theorem 2. Π_{WA} securely realizes \mathcal{F}_{WA} with abort, in the presence of one malicious party in the $(\mathcal{F}_{Mult}, \mathcal{F}_{PC}, \mathcal{F}_{Reconst}, \mathcal{F}_{Prep})$ -hybrid model.

Proof. We use a similar set-up as the proof of Theorem 1. Step 1 is local computation and does not need simulation. Steps 2, 4 can be simulated using the simulators for $\mathcal{F}_{Reconst}$, \mathcal{F}_{PC} respectively. Input extraction follows from having access to r_i (through \mathcal{F}_{Prep}) and output x if the protocol does not abort. Finally, if the protocol does abort at any time in the internal run, then the simulator sends Abort to \mathcal{F}_{WA} . Otherwise, it simply passes on the extracted shares of $a[i]$ to \mathcal{F}_{WA} and the honest parties receive their outputs. Note that Π_{DReLU} is not formally defined. However, this is simply local computation over Π_{WA} and the proofs can be extended analogously. \square

³For more details on these, refer to [25]

Theorem 3. Π_{ReLU} securely realizes $\mathcal{F}_{\text{ReLU}}$ with abort, in the presence of one malicious party in the $(\mathcal{F}_{\text{Mult}}, \mathcal{F}_{\text{WA}}, \mathcal{F}_{\text{Prep}})$ -hybrid model.

Proof. Simulation is done as before using the hybrid argument. The protocol simply composes \mathcal{F}_{WA} and $\mathcal{F}_{\text{Mult}}$ and hence is simulated using the corresponding simulators. \square

Theorem 4. Π_{Maxpool} securely realizes $\mathcal{F}_{\text{Maxpool}}$ with abort, in the presence of one malicious party in the $(\mathcal{F}_{\text{Mult}}, \mathcal{F}_{\text{ReLU}}, \mathcal{F}_{\text{Prep}})$ -hybrid model.

Proof. Similar to the proof of Theorem 3, simulation works by sequentially composing the simulators for $\mathcal{F}_{\text{ReLU}}$ and $\mathcal{F}_{\text{Mult}}$. \square

Theorem 5. Π_{Pow} securely realizes \mathcal{F}_{Pow} with abort, in the presence of one malicious party in the $(\mathcal{F}_{\text{Mult}}, \mathcal{F}_{\text{ReLU}}, \mathcal{F}_{\text{Reconst}}, \mathcal{F}_{\text{Prep}})$ -hybrid model.

Proof. The simulator for \mathcal{A} works by playing the role of the trusted party for $\mathcal{F}_{\text{Mult}}$, $\mathcal{F}_{\text{ReLU}}$, and $\mathcal{F}_{\text{Reconst}}$. The protocol sequentially reveals bits of the scale α . It is important to note the functionality that it emulates (see in Fig. 13). The simulator runs the first iteration of the loop and in the process extracts the adversaries inputs. Then it proceeds to complete all the iterations of the loop. If the protocol proceeds without aborting till the end, then the simulator sends the extracted shares of b along with $k = 0$ to the functionality \mathcal{F}_{Pow} . If the protocol aborts at iteration k , then the simulator sends the extracted shares of b along with k to \mathcal{F}_{Pow} . \square

Theorem 6. $\Pi_{\text{Div}}, \Pi_{\text{BN}}$ securely realize $\mathcal{F}_{\text{Div}}, \mathcal{F}_{\text{BN}}$ respectively, with abort, in the presence of one malicious party in the $(\mathcal{F}_{\text{Mult}}, \mathcal{F}_{\text{Pow}}, \mathcal{F}_{\text{Prep}})$ -hybrid model.

Proof. $\Pi_{\text{Div}}, \Pi_{\text{BN}}$ are sequential combinations of local computations and invocations of $\mathcal{F}_{\text{Mult}}$. Simulation follows directly from composing the simulators and input extraction follows from the simulator of Π_{Pow} . \square

Protocol Overheads. We theoretically estimate the overheads of our protocols in Table 6 in Appendix A. The dominant round complexity for private compare comes from the string multiplication in Step 6. wrap_3 requires one additional round and one additional ring element (two in malicious security) over private compare. Computing derivative of ReLU is a local computation over the wrap_3 function. Computing ReLU requires two additional rounds and one ring element (two for malicious)⁴. Maxpool and derivative of require rounds proportional to the area of the filter. Finally, pow, division, and batch-norm requires a quadratic number of rounds in ℓ .

⁴And one (two) additional bits.

5 Experimental Evaluation

We evaluate the performance of training and inference with FALCON on 6 networks of varying parameter sizes trained using MNIST, CIFAR-10 and Tiny ImageNet datasets (cf. Appendix C). A number of prior works such as SecureML [6], DeepSecure [32], MiniONN [19], Gazelle [10], SecureNN [7], ABY³ [8], and Chameleon [11] evaluate over one or more of these networks and we mimic their evaluation set-up for comparison.

5.1 Experimental Setup

We implement FALCON framework in about 12.3k LOC in C++ using the communication backend of SecureNN⁵. We run our experiments on Amazon EC2 machines over Ubuntu 16.04 LTS with Intel-Core i7 processor and 64GB of RAM. Our evaluation set-up uses similar or poorer hardware as compared to prior work [6–8, 10, 11]. We perform extensive evaluation of our framework in both the LAN and WAN setting. For the LAN setting, our bandwidth is about 625 MBps and ping time is about 0.2ms. For WAN experiments, we run servers in different geographic regions with 70ms ping time and 40 MBps bandwidth.

Optimizations: All data-independent computation, i.e., pre-computation, is parallelized using 16 cores to reduce the run-time. When a ReLU layer is followed by a Maxpool layer, we swap the order of these two layers for optimized runtimes. We use the Eigen library for faster matrix multiplication and parallelize the private compare computation. We optimize across the forward and backward pass for Maxpool, ReLU, and Batch-Normalization layers, i.e., we compute the relevant derivatives while computing the functions. We use 32-bit integer range with 16 bits of floating point precision. As the entire codebase is parallelizable, in the future, significant improvement is possible by implementing FALCON using TensorFlow or PyTorch which support easy parallelization as well as computations over GPUs.

5.2 Networks

We evaluate FALCON on the following popular deep learning networks. We select these networks based on the varied range of model parameters and different types of layers used in the network architecture. The first three networks are purposely selected to perform performance comparison of FALCON with prior work that evaluated on these models. The number of layers that we report include only convolutional and fully connected layers. We provide a detailed configuration for each of the networks in Appendix D. We also note that we enable the exact same functionality as prior work with no further approximations. Our networks thus achieve an accuracy of 99.15% on Network C, 98.77% on Network B, and

⁵<https://github.com/snwagh/securenn-public>

93.4% on Network A – same as the accuracy for SecureNN, SecureML, and ABY³ [6–8].

- (A) **Network-A:** This is a 3-layered fully-connected network with ReLU activation after each layer as was evaluated in SecureML [6] (see Figure 3). This is the smallest network with around 118K parameters.
- (B) **Network-B:** This network again is a 3-layered network with the first layer as convolution followed by 2 fully-connected layers using ReLU activation after each layer. This architecture is chosen from Chameleon [11] with approximately 100K parameters (see Figure 8).
- (C) **Network-C:** This is a 4-layered network with 2 convolutional and 2 fully-connected layers selected from prior work MiniONN [19]. This network uses Max Pooling in addition to ReLU layer and has around 10,500 parameters in total (shown in Figure 5).
- (D) **LeNet:** This network, first proposed by LeCun et al. [33] was used in automated detection of zip codes and digit recognition [34]. The network contains 2 convolutional layers and 2 fully connected layers with 431K parameters (shown in Figure 7).
- (E) **AlexNet:** AlexNet is the famous winner of the 2012 ImageNet ILSVRC-2012 competition [15]. It has 5 convolutional layers and 3 fully connected layers and uses Batch-Normalization layer for stability, efficient training and has about 60 Million parameters (see Figure 6). FALCON is the first private deep learning framework that evaluates AlexNet because of the support for Batch-Normalization layer in our system.
- (F) **VGG16:** The last network which we implement is called VGG16, the runner-up of the ILSVRC-2014 competition [14]. VGG16 has 16 layers and has about 138 Million parameters (see Figure 4).

5.3 Results for Private Inference

Tables 2, 3 report the end-to-end latency time (in seconds) and number of bytes (in MB) communicated for performing a single inference query with FALCON. We compare these values with the numbers reported from prior work wherever applicable. All the numbers are reported for both semi-honest and malicious adversarial setting. Further, we execute the queries in both LAN and WAN setting using FALCON.

Comparison to Prior Work. We compare the inference time of a single query and the communication bytes of FALCON with prior work on networks A, B and C. None of the prior works evaluate the remaining networks and hence we do not compare the performance of FALCON for the networks in Table 3⁶. Depending on the network architecture, our results

⁶XONN evaluates on binarized model parameters of VGG16 and hence we do not compare with it.

are between $3\times$ - $120\times$ faster than existing work. In particular, we are upto $18\times$ faster than XONN [9] ($11\times$ on average) and $32\times$ faster than Gazelle ($23\times$ on average), $8\times$ faster than SecureNN ($3\times$ on average), and comparable to ABY³ on small networks. We are also $40\times$ more communication efficient than ABY³ [8], $200\times$ more communication efficient than SecureNN [7], and over $760\times$ more communication efficient compared to XONN [9].

Inference time and communication with FALCON. For both the adversarial settings, the inference latency for FALCON over LAN is within 25ms for smaller networks (A and B) and around 100ms for Network-C and LeNet. For AlexNet and VGG16, the inference time ranges from 0.5 to 12s depending on the model and the input dataset. The inference time increases with the size of the input image. Hence, queries over Tiny ImageNet are slower than CIFAR-10 for the same model architecture. The inference time over the WAN setting ranges from 1 to 3s for the networks A, B and C and from 3 to 37s for the remaining larger networks. However, we emphasize that the inference time with semi-honest adversarial setting is around $3\times$ faster than that for the malicious adversary. Hence, a faster deployment protocol is possible depending on the trust assumptions of the application.

In addition to efficient response times, our results show that FALCON is optimized for communication rounds as well. The parties exchange less than 4MB of data for smaller networks (Table 2) and 5MB to 400MB for larger networks (Table 3). The amount of data exchanged is the same for both the LAN and WAN setting. However, similar to the inference time, more communication bytes are required for the malicious setting as compared to the semi-honest adversary.

5.4 Results for Private Training

Tables 4, 5 report the execution time and the communication required for training all the 6 network architectures.

Comparison to Prior Work. For private training, FALCON is upto $6\times$ faster than SecureNN [7] ($4\times$ on average), $4.4\times$ faster than ABY³ and $70\times$ faster than SecureML [6]. We highlight that FALCON achieves these speedups due to improved protocols (both round complexity and communication as described in Section 2.3). As seen from Table 4, the communication overhead is $10\times$ to $100\times$ better for FALCON as compared to other solutions.

Execution time for FALCON. The time to privately train networks A, B and C with FALCON is around 3 to 40 hrs. For larger networks, we extrapolate time from a single iteration of a forward and a backward pass. The training time ranges from a few weeks to hundreds of weeks. Although these values seem to be quite large, high capacity machine learning models are known to take from a few days to weeks to achieve high accuracy when trained (both on CPU as well as GPU). Such networks can also benefit from transfer learning techniques,

	Framework	Adversarial Setting	LAN/WAN	Network-A		Network-B		Network-C	
				Time	Comm.	Time	Comm.	Time	Comm.
2PC	SecureML [6]	Semi-honest	LAN	4.88	-	-	-	-	-
	DeepSecure [32]	Semi-honest	LAN	-	-	9.67	791	-	-
	EzPC [20]	Semi-honest	LAN	0.7	76	0.6	70	5.1	501
	Gazelle [10]	Semi-honest	LAN	0.09	0.5	0.29	0.8	1.16	70
	MiniONN [19]	Semi-honest	LAN	1.04	15.8	1.28	47.6	9.32	657.5
	XONN [9]	Semi-honest	LAN	0.13	4.29	0.16	38.3	0.15	32.1
3PC	Chameleon [11]	Semi-honest	LAN	-	-	2.7	12.9	-	-
	ABY ³ [8]	Semi-honest	LAN	0.008	0.5	0.01	5.2	-	-
	SecureNN [7]	Semi-honest	LAN	0.043	2.1	0.076	4.05	0.13	8.86
	FALCON	Semi-honest	LAN	0.011	0.012	0.009	0.049	0.042	0.51
		Malicious	LAN	0.021	0.31	0.022	0.52	0.089	3.37
	SecureNN [7]	Semi-honest	WAN	2.43	2.1	3.06	4.05	3.93	8.86
	FALCON	Semi-honest	WAN	0.99	0.012	0.76	0.049	3.0	0.5
		Malicious	WAN	2.33	0.31	1.7	0.52	7.8	3.37

Table 2: Comparison of inference time of various frameworks for different networks using MNIST dataset. All runtimes are reported in seconds and communication in MB. ABY³ and XONN do not implement their maliciously secure versions. 2-party (2PC) protocols are presented here solely for the sake of comprehensive evaluation of the literature.

Framework	Adversarial Setting	LAN/WAN	LeNet (MNIST)		AlexNet (CIFAR-10)		VGG16 (CIFAR-10)		AlexNet (ImageNet)		VGG16 (ImageNet)	
			Time	Comm.	Time	Comm.	Time	Comm.	Time	Comm.	Time	Comm.
FALCON	Semi-honest	LAN	0.047	0.74	0.17	1.35	1.91	13.51	2.03	19.22	3.15	52.56
	Malicious	LAN	0.12	5.69	0.53	16.5	7.91	164.9	7.86	160.4	12.04	395.7
	Semi-honest	WAN	3.06	0.74	8.9	1.35	11.82	13.51	8.62	19.22	12.96	52.56
	Malicious	WAN	7.87	5.69	21.9	16.5	33.03	164.9	24.76	160.4	37.6	395.7

Table 3: Comparison of inference time of various frameworks over popular benchmarking network architectures from the machine learning domain. All runtimes are reported in seconds and communication in MB.

where a public pre-trained model is fine-tuned with a private dataset. This fine-tuning requires fewer epochs and hence can speed up the overall runtime considerably.

5.5 Compute vs. Communication Cost

Figure 2 shows the computation time as compared to the communication time for the inference of a single input over different network sizes. We observe that the computation cost increases with the network size and becomes the dominant reason for the performance overhead in private deep learning with FALCON. This observation is against the conventional wisdom that MPC protocols are communication bound and not computation bound. When running larger networks such as AlexNet and VGG16, and especially for Tiny ImageNet, the computation time starts becoming a significant fraction of the total time. Hence, we claim that FALCON is optimized for communication rounds, specifically when operating over large networks. With our results, we motivate the community to focus on designing faster compute solutions using accelerators such as GPUs, parallelization, efficient matrix multiplications and caching, along with the conventional goals of reducing communication and round complexity.

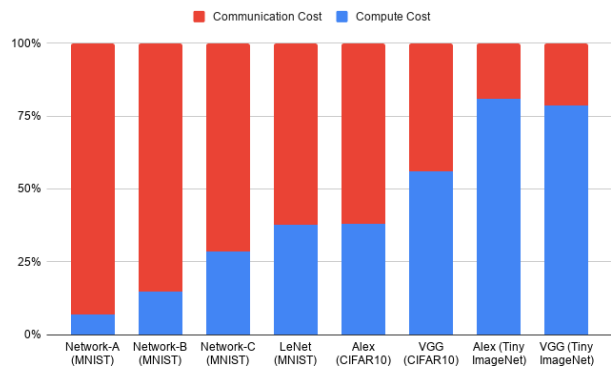


Figure 2: Computation vs. communication cost for private inference using FALCON in a WAN deployment for the malicious adversary setting. It is interesting to note that as the network size increases, computation becomes a dominant factor in the overall end-to-end runtime.

5.6 Comparison with Plaintext Computation

We compare our private deep learning overheads with plaintext execution of the same networks. Our findings indicate that private deep learning (over CPU) is within a factor of 6× of cleartext execution of the same network over CPU and within 60× that of cleartext execution over GPU (using PyTorch). For instance, a single epoch for AlexNet (batch size 128) over CPU using privacy-preserving techniques requires about 3,200s and the same setting in the clear requires 570s over CPU. However, using GPUs, the same network requires

Framework	Adversarial Setting	LAN/WAN	Network-A		Network-B		Network-C	
			Time	Comm.	Time	Comm.	Time	Comm.
SecureML [6]*	Semi-honest	LAN	81.7	-	-	-	-	-
SecureML [6]	Semi-honest	LAN	7.02	-	-	-	-	-
ABY ³ [8]	Semi-honest	LAN	0.75	0.031	-	-	-	-
SecureNN [7]	Semi-honest	LAN	1.03	0.11	-	-	17.4	30.6
FALCON	Semi-honest	LAN	0.17	0.016	0.42	0.056	3.71	0.54
	Malicious	LAN	0.56	0.088	1.17	0.32	11.9	3.29
SecureML [6]*	Semi-honest	WAN	4336	-	-	-	-	-
SecureNN [7]	Semi-honest	WAN	7.83	0.11	-	-	53.98	30.6
FALCON	Semi-honest	WAN	3.76	0.016	3.4	56.14	14.8	0.54
	Malicious	WAN	8.01	0.088	7.5	0.32	39.32	3.29
Batch Size, Epochs			128, 15		128, 15		128, 15	

Table 4: Comparison of training time of various frameworks over popular benchmarking network architectures from the security domain. All runtimes are reported in hours and communication in TB. * correspond to 2PC numbers. ABY³ does not implement their maliciously secure protocols.

Framework	Adversarial Setting	LAN/WAN	LeNet		AlexNet (CIFAR-10)		VGG16 (CIFAR-10)		AlexNet (ImageNet)		VGG16 (ImageNet)	
			Time	Comm.	Time	Comm.	Time	Comm.	Time	Comm.	Time	Comm.
FALCON	Semi-honest	LAN	0.036	0.81	0.47	7.24	5.02	45.9	73.0	222.9	30.9	156.0
	Malicious	LAN	0.73	4.82	1.68	43.4	18.18	185.3	276	1598	116	1012
	Semi-honest	WAN	0.11	0.81	1.39	7.24	12.44	45.9	91.7	222.9	41.0	156.0
	Malicious	WAN	0.31	4.82	4.31	43.4	31.32	185.3	340	1598	147	1012
Batch Size, Epochs			128, 15		128, 90		128, 25		128, 90		128, 25	

Table 5: Comparison of training time of various frameworks over popular benchmarking network architectures from the machine learning domain. All runtimes are reported in weeks and communication in TB.

about 57s for a single epoch. This shows the importance of supporting GPUs and optimizers for private deep learning.

6 Related Work

Privacy-preserving training: In a seminal paper on private machine learning, Mohassel *et al.* [6] show protocols for a variety of machine learning algorithms such as linear regression, logistic regression and neural networks. Their approach is based on a 2-party computation model and rely on techniques such as oblivious transfer [37] and garbled circuits [4]. Following that, Mohassel *et al.* [8] proposed a new framework called ABY³ which generalizes and optimizes switching back and forth between arithmetic, binary, and Yao garbled circuits in a 3-party computation model. Wagh *et al.* [7] proposed SecureNN that considers a similar 3-party model with semi-honest security and eliminate expensive cryptographic operations to demonstrate privacy-preserving training and inference of neural networks. SecureNN also provides *malicious privacy*, a notion formalized by Araki *et al.* [21] but not correctness in the presence of malicious corruption. FALCON provides a holistic framework for both training and inference of neural networks while improving computation and communication overhead as compared to prior work.

Privacy-preserving inference: Privacy-preserving inference has received considerable attention over the last few years. Recall that we have summarized some of these works in Table 1. Private inference typically relies on one or more

of the following techniques: secret sharing [7, 8], garbled circuits [9, 20], homomorphic encryption [6, 19] or Goldreich-Micali-Wigderson (GMW) [11, 29], each with its own advantages and disadvantages. CryptoNets [12] was one of the earliest works to demonstrate the use of homomorphic encryption to perform private inference. CryptoDL [38] developed techniques that use approximate, low-degree polynomials to implement non-linear functions and improve on CryptoNets. DeepSecure [32] uses garbled circuits to develop a privacy-preserving deep learning framework.

Chameleon [11] is another mixed protocol framework that uses the Goldreich-Micali-Wigderson (GMW) protocol [29] for low-depth non-linear functions, garbled circuits for high-depth functions and secret sharing for linear operations to achieve high performance gains. The above three [6, 8, 11] demonstrate private machine learning for other machine learning algorithms such as SVMs, linear and logistic regression as well. Gazelle [10] combines techniques from homomorphic encryption with MPC and optimally balances the use of a specially designed linear algebra kernel with garbled circuits to achieve fast private inference. EzPC [20] is a ABY-based [39] secure computation framework that translates high-level programs into Boolean and arithmetic circuits. Riazi *et al.* propose a framework XONN [9] and showcase compelling performance for inference on large *binarized* neural networks. XONN [9] uses garbled circuits to provide constant round private inference. The work also provides a simple easy-to-use API with a translator from Keras [40] to XONN. EPIC [41] demonstrates the use of

transfer learning in the space of privacy-preserving machine learning while Quotient [42] takes the first steps in developing two party secure computation protocols for optimizers and normalizations. Recent works [43, 44] explore a stronger adversarial model called guaranteed output delivery in a similar 3 party honest majority corruption model. Another line of work aims at designing protocols in a “dishonest-majority” adversarial model. Here, $n - 1$ out of the n computing parties can be corrupted. Seminal works in this line of research are BDOZa [45] and SPDZ [46]. Helen [47] allows distributed training of linear models while preserving privacy.

7 Conclusion

In this work, we develop new protocols for private training and inference in a honest-majority 3-party setting. Theoretically, we propose novel protocols that improve the round and communication complexity and provide security against maliciously corrupt adversaries with an honest majority. FALCON thus provides malicious security and provides several orders of magnitude performance improvements over prior work. Experimentally, FALCON is the first secure deep learning framework to examine performance over large-scale networks such as AlexNet and VGG16 and over large-scale datasets such as Tiny ImageNet. We also are the first work to demonstrate efficient protocols for batch-normalization which is a critical component of present day machine learning.

References

- [1] E. Bursztein, E. Clarke, M. DeLaune, D. M. Eliff, N. Hsu, L. Olson, J. Shehan, M. Thakur, K. Thomas, and T. Bright, “Rethinking the detection of child sexual abuse imagery on the internet,” in *The World Wide Web Conference*. ACM, 2019, pp. 2601–2607.
- [2] “Child abusers run rampant as tech companies look the other way,” 2019. [Online]. Available: <https://www.nytimes.com/interactive/2019/11/09/us/internet-child-sex-abuse.html>
- [3] H. Cho, D. J. Wu, and B. Berger, “Secure genome-wide association analysis using multiparty computation,” *Nature biotechnology*, vol. 36, no. 6, p. 547, 2018.
- [4] A. C. Yao, “Protocols for secure computations,” in *IEEE FOCS*, 1982.
- [5] A. Shamir, “How to share a secret,” *Communications of the ACM*, vol. 22, no. 11, pp. 612–613, 1979.
- [6] P. Mohassel and Y. Zhang, “SecureML: A system for scalable privacy-preserving machine learning,” in *IEEE Symposium on Security and Privacy (S&P)*, 2017.
- [7] S. Wagh, D. Gupta, and N. Chandran, “SecureNN: 3-Party Secure Computation for Neural Network Training,” *Privacy Enhancing Technologies Symposium (PETS)*, 2019.
- [8] P. Mohassel and P. Rindal, “ABY³: A mixed protocol framework for machine learning,” in *ACM Conference on Computer and Communications Security (CCS)*, 2018.
- [9] M. S. Riazi, M. Samragh, H. Chen, K. Laine, K. Lauter, and F. Koushanfar, “XONN: XNOR-based Oblivious Deep Neural Network Inference,” in *USENIX Security Symposium*, 2019.
- [10] C. Juvekar, V. Vaikuntanathan, and A. Chandrakasan, “Gazelle: A low latency framework for secure neural network inference,” in *USENIX Security Symposium*, 2018.
- [11] M. S. Riazi, C. Weinert, O. Tkachenko, E. M. Songhori, T. Schneider, and F. Koushanfar, “Chameleon: A hybrid secure computation framework for machine learning applications,” in *ACM Symposium on Information, Computer and Communications Security (ASIACCS)*, 2018.
- [12] R. Gilad-Bachrach, N. Dowlin, K. Laine, K. E. Lauter, M. Naehrig, and J. Wernsing, “CryptoNets: Applying neural networks to encrypted data with high throughput and accuracy,” in *ICML*, 2016.
- [13] J. Furukawa, Y. Lindell, A. Nof, and O. Weinstein, “High-throughput secure three-party computation for malicious adversaries and an honest majority,” in *Advances in Cryptology—EUROCRYPT*, 2017.
- [14] K. Simonyan and A. Zisserman, “Very deep convolutional networks for large-scale image recognition,” *arXiv preprint arXiv:1409.1556*, 2014.
- [15] A. Krizhevsky, I. Sutskever, and G. E. Hinton, “Imagenet classification with deep convolutional neural networks,” in *Advances in Neural Information Processing Systems*, 2012, pp. 1097–1105.
- [16] “MNIST database,” <http://yann.lecun.com/exdb/mnist/>, accessed: 2017-09-24.
- [17] A. Krizhevsky, V. Nair, and G. Hinton, “The CIFAR-10 dataset,” URL: <http://www.cs.toronto.edu/kriz/cifar.html>, 2014.
- [18] J. Wu, Q. Zhang, and G. Xu, “Tiny ImageNet Challenge.” [Online]. Available: <http://cs231n.stanford.edu/reports/2017/pdfs/930.pdf>
- [19] J. Liu, M. Juuti, Y. Lu, and N. Asokan, “Oblivious neural network predictions via MiniONN transformations,” in

ACM Conference on Computer and Communications Security (CCS), 2017.

- [20] N. Chandran, D. Gupta, A. Rastogi, R. Sharma, and S. Tripathi, “EzPC: programmable, efficient, and scalable secure two-party computation for machine learning,” *Cryptology ePrint Archive*, Report 2017/1109. <https://eprint.iacr.org/2017/1109>, Tech. Rep., 2017.
- [21] T. Araki, J. Furukawa, Y. Lindell, A. Nof, and K. Ohara, “High-throughput semi-honest secure three-party computation with an honest majority,” in *ACM Conference on Computer and Communications Security (CCS)*, 2016.
- [22] R. Shokri, M. Stronati, C. Song, and V. Shmatikov, “Membership inference attacks against machine learning models,” in *IEEE Symposium on Security and Privacy (S&P)*, 2017.
- [23] M. Fredrikson, S. Jha, and T. Ristenpart, “Model inversion attacks that exploit confidence information and basic countermeasures,” in *ACM Conference on Computer and Communications Security (CCS)*. ACM, 2015.
- [24] F. Tramèr, F. Zhang, A. Juels, M. K. Reiter, and T. Ristenpart, “Stealing machine learning models via prediction APIs,” in *USENIX Security Symposium*, 2016.
- [25] E. Kushilevitz, Y. Lindell, and T. Rabin, “Information-theoretically secure protocols and security under composition,” *SIAM Journal on Computing*, vol. 39, no. 5, pp. 2090–2112, 2010.
- [26] S. Ioffe and C. Szegedy, “Batch normalization: Accelerating deep network training by reducing internal covariate shift,” in *Proceedings of the International Conference on Machine Learning*, 2015, pp. 448–456.
- [27] O. Catrina and A. Saxena, “Secure computation with fixed-point numbers,” in *International Conference on Financial Cryptography and Data Security*, 2010, pp. 35–50.
- [28] M. Aliasgari, M. Blanton, Y. Zhang, and A. Steele, “Secure computation on floating point numbers,” in *Symposium on Network and Distributed System Security (NDSS)*, 2013.
- [29] O. Goldreich, S. Micali, and A. Wigderson, “How to play any mental game or a completeness theorem for protocols with honest majority,” in *ACM Symposium on Theory of Computing (STOC)*, 1987.
- [30] R. Canetti, “Security and composition of multiparty cryptographic protocols,” *Journal of CRYPTOLOGY*, vol. 13, no. 1, pp. 143–202, 2000.
- [31] —, “Universally composable security: A new paradigm for cryptographic protocols,” in *Proceedings of the 42Nd IEEE Symposium on Foundations of Computer Science*, ser. FOCS ’01, 2001, pp. 136–.
- [32] B. D. Rouhani, M. S. Riazi, and F. Koushanfar, “DeepSecure: Scalable Provably-Secure Deep Learning,” *IACR Cryptology ePrint Archive*, vol. 2017, p. 502, 2017.
- [33] Y. LeCun, L. Bottou, Y. Bengio, and P. Haffner, “Gradient-based learning applied to document recognition,” *Proceedings of the IEEE*, vol. 86, no. 11, pp. 2278–2324, 1998.
- [34] Y. LeCun, B. Boser, J. S. Denker, D. Henderson, R. E. Howard, W. Hubbard, and L. D. Jackel, “Backpropagation applied to handwritten zip code recognition,” *Neural computation*, vol. 1, no. 4, pp. 541–551, 1989.
- [35] Y. Lindell and B. Pinkas, “Privacy preserving data mining,” in *Annual International Cryptology Conference*. Springer, 2000, pp. 36–54.
- [36] R. Bost, R. A. Popa, S. Tu, and S. Goldwasser, “Machine learning classification over encrypted data,” in *Symposium on Network and Distributed System Security (NDSS)*, 2015.
- [37] C. Peikert, V. Vaikuntanathan, and B. Waters, “A framework for efficient and composable oblivious transfer,” in *Advances in Cryptology—CRYPTO*, 2008.
- [38] E. Hesamifard, H. Takabi, and M. Ghasemi, “CryptoDL: Deep Neural Networks over Encrypted Data,” in *Privacy Enhancing Technologies Symposium (PETS)*, 2018.
- [39] D. Demmler, T. Schneider, and M. Zohner, “ABY – A framework for efficient mixed-protocol secure two-party computation,” in *Symposium on Network and Distributed System Security (NDSS)*, 2015.
- [40] F. Chollet *et al.*, “Keras,” <https://github.com/fchollet/keras>, 2015.
- [41] E. Makri, D. Rotaru, N. P. Smart, and F. Vercauteren, “EPIC: efficient private image classification (or: learning from the masters),” in *Cryptographers’ Track at the RSA Conference*. Springer, 2019, pp. 473–492.
- [42] N. Agrawal, A. Shahin Shamsabadi, M. J. Kusner, and A. Gascón, “Quotient: Two-party secure neural network training and prediction,” in *ACM Conference on Computer and Communications Security (CCS)*. ACM, 2019, pp. 1231–1247.
- [43] E. Boyle, N. Gilboa, Y. Ishai, and A. Nof, “Practical Fully Secure Three-Party Computation via Sublinear Distributed Zero-Knowledge Proofs,” in

ACM Conference on Computer and Communications Security (CCS), 2019. [Online]. Available: <http://doi.acm.org/10.1145/3319535.3363227>

- [44] D. Boneh, E. Boyle, H. Corrigan-Gibbs, N. Gilboa, and Y. Ishai, “Zero-Knowledge Proofs on Secret-Shared Data via Fully Linear PCPs,” in *Advances in Cryptology—CRYPTO*. Springer, 2019, pp. 67–97.
- [45] R. Bendlin, I. Damgård, C. Orlandi, and S. Zakarias, “Semi-homomorphic encryption and multiparty computation,” in *Annual International Conference on the Theory and Applications of Cryptographic Techniques*. Springer, 2011, pp. 169–188.
- [46] I. Damgård, V. Pastro, N. Smart, and S. Zakarias, “Multiparty computation from somewhat homomorphic encryption,” in *Annual Cryptology Conference*. Springer, 2012, pp. 643–662.
- [47] W. Zheng, R. A. Popa, J. E. Gonzalez, and I. Stoica, “Helen: Maliciously Secure Cooperative Learning for Linear Models,” in *IEEE Symposium on Security and Privacy (S&P)*, 2019.

A Theoretical Complexity of FALCON

We theoretically estimate the overheads of our protocols in Table 6. The dominant round complexity for private compare comes from the string multiplication in Step 6. `wrap3` requires one additional round and one additional ring element (two in malicious security) over private compare. Computing derivative of ReLU is a local computation over the `wrap3` function. Computing ReLU requires two additional rounds and one ring element (two for malicious)⁷. Maxpool and derivative of require rounds proportional to the area of the filter. Finally, pow, division, and batch-norm require a quadratic number of rounds in ℓ .

B Neural Networks

We present a brief summary of neural networks as well as the our evaluation benchmarks. Neural Networks, in particular Convolutional Neural Networks (CNN) form the state-of-the-art techniques for image classification. The operation of neural networks is most widely based on stochastic gradient descent and usually iterates over the following three components: a forward pass, a backward pass and a parameter update phase.

A neural network architecture is defined by the combination of layers that compose the network. Various types of layers such as convolution, fully connected, pooling layers, and activation functions are used in different combinations

⁷And one (two) additional bits.

to form the network. In the training phase, a neural network takes in a batch of inputs and outputs “a guess” (forward pass). The ground truth is then used to compute errors using chain rule (back-prop) and finally update the network parameters (update phase). In the inference phase, the output of the forward pass is used for prediction purposes. Below we look at the various components required by state-of-the-art neural networks.

Our general framework supports the following types of layers: convolutional, fully connected, pooling layers (max and mean pooling), normalization layers and the ReLU activation function. Together these enable a vast majority of networks used in machine learning literature. In the forward pass, each layer takes in an input from the previous layer and generates the output (input for the following layer) using learnable parameters such as weights, biases etc. The final layer output is used to then compute the loss using a loss function (such as cross-entropy, mean squared etc.). In the backward pass, the final layer loss is propagated backwards through each layer using the chain rule. Finally, each layer uses the associated loss to update its learnable parameters. Below we look at each layer in detail. We use Einstein tensor notation with ϵ_{ab} to denote the Kronecker Delta (to avoid confusion with the error δ) to describe each layer.

B.1 Convolutional Layer

The input to a convolution layer is a 4D tensor $\mathbb{R}^{w_{in}, h_{in}, D_{in}, B}$ where w_{in}, h_{in} are the width and height of the input, D_{in} is the number of input filters and B is the batch size. The hyper-parameters are the number of output filters D_{out} , the filter size F , the stride S and the amount of zero padding P . The output of the layer is another 4D tensor $\mathbb{R}^{w_{out}, h_{out}, D_{out}, B}$ where $w_{out} = (w_{in} - F + 2 * P) / S + 1$ and $h_{out} = (h_{in} - F + 2 * P) / S + 1$. The weights are 4D tensors in $\mathbb{R}^{F, F, D_{in}, D_{out}}$ and biases are a vector in $\mathbb{R}^{D_{out}}$.

The forward pass is simply a convolution between the inputs activation and the weights plus the bias. The backward pass as well as the update equations are also convolutions which can all be implemented as matrix multiplications. We use the following notation: activations are represented by a^l and indexed by the layer number $l \in \{1 \dots L\}$, δ^l represents $\frac{\partial C}{\partial a^l}$, the error of layer l , weights and biases are represented by w and b . Dimension variables are: $\alpha \in \{1, \dots, w_{in}\}, \beta \in \{1, \dots, h_{in}\}, r \in \{1, \dots, D_{in}\}, d \in \{1, \dots, D_{out}\}, b \in \{1, \dots, B\}, x \in \{1, \dots, w_{out}\}$, and $y \in \{1, \dots, h_{out}\}$

	Protocol	Dependence	Semi-Honest		Malicious	
			Rounds	Comm	Rounds	Comm
Basic Protocols	MatMul	$(x \times y)(y \times z)$	1	kxz	1	$2kxz$
	Private Compare	n	$2 + \log_2 \ell$	$2kn$	$\ell + 2$	$4kn$
	wrap ₃	n	$3 + \log_2 \ell$	$3kn$	$\ell + 3$	$6kn$
Compound Protocols	ReLU and Derivative of ReLU	n	$5 + \log_2 \ell$	$4kn$	$\ell + 5$	$8kn$
	MaxPool and Derivative of Maxpool	$n, \{w, h\}$	$(wh - 1)(7 + \log_2 \ell)$	$5k + wh$	$(wh - 1)(7 + \log_2 \ell)$	$10k + 2wh$
	Pow	n	$5\ell + \ell \cdot \log_2 \ell$	$4kn\ell$	$5\ell + \ell \cdot \log_2 \ell$	$8kn\ell$
	Division	n	$7 + 5\ell + \ell \cdot \log_2 \ell$	$4kn\ell + 7kn$	$7 + 5\ell + \ell \cdot \log_2 \ell$	$8kn\ell + 14kn$
	Batch Norm	r, n	$15 + 5\ell + \ell \cdot \log_2 \ell$	$kr + 4kr\ell + 14krn$	$15 + 5\ell + \ell \cdot \log_2 \ell$	$2kr + 8kr\ell + 28krn$

Table 6: Theoretical overheads of basic and compound protocols. Communication is in Bytes where ℓ is the logarithm of the ring size and k is its Byte size. We use n to denote the size of the vector in vectorized implementations.

$$a_{x,y,d,b}^l = w_{p,q,r,d} \cdot a_{(xS-P+p),(yS-P+q),r,b}^{l-1} + b_d \quad (14a)$$

$$\delta_{\alpha,\beta,r,b}^{l-1} = \delta_{x,y,d,b}^l \cdot w_{(\alpha+P-xS),(\beta+P-yS),r,d} \quad (14b)$$

$$\frac{\partial C}{\partial w_{p,q,r,d}} = a_{(xS-P+p),(yS-P+q),r,b}^{l-1} \cdot \delta_{x,y,d,b}^l \quad (14c)$$

$$\frac{\partial C}{\partial b_d} = \delta_{x',y',d,b'}^l \cdot \epsilon_{xx'} \epsilon_{yy'} \epsilon_{bb'} \quad (14d)$$

Equation 14a is used for the forward pass, equation 14b is used for back-prop, and equations 14c, 14d are used for updating layer parameters.

B.2 Fully Connected Layer

The input to a convolution layer is a matrix in $\mathbb{R}^{c_{in},B}$ where B is the batch size. The layer is defined by the number of input and output channels c_{in}, c_{out} . The output of the layer is a matrix in $\mathbb{R}^{c_{in},B}$. The weights are a matrix in $\mathbb{R}^{c_{in},c_{out}}$ and biases form a vector of size $\mathbb{R}^{c_{out}}$.

The forward pass is a matrix multiplication of the input matrix with the weights matrix and bias added. The backward pass as well as the update equations require matrix multiplications. Using the notation as in the convolutional layer, the equations defining the fully connected layer are described as follows:

$$a_{y,b}^l = w_{p,y} \cdot a_{p,b}^{l-1} + b_y \quad (15a)$$

$$\delta_{x,b}^{l-1} = \delta_{y,b}^l \cdot w_{x,y} \quad (15b)$$

$$\frac{\partial C}{\partial w_{p,q}} = a_{p,b}^{l-1} \cdot \delta_{q,b}^l \quad (15c)$$

$$\frac{\partial C}{\partial b_y} = \delta_{y,b'}^l \cdot \epsilon_{bb'} \quad (15d)$$

Equation 15a is used for the forward pass, equation 15b is used for back-prop, and equations 15c, 15d are used for updating layer parameters.

B.3 Pooling Layer

The input to a pooling layer (specifically Maxpool) is a 4D tensor $\mathbb{R}^{w_{in},h_{in},D_{in},B}$ where w_{in}, h_{in} are the width and height of the input, D_{in} the number of input filters and B the batch size. The hyper-parameters are the filter size F and the stride S . The output of the layer is another 4D tensor $\mathbb{R}^{w_{out},h_{out},D_{in},B}$ where $w_{out} = (w_{in} - F)/S + 1$ and $h_{out} = (h_{in} - F)/S + 1$. There are no learnable parameters as the output is a fixed function of the input.

The forward pass is max operation over the filter and can be implemented using sequential comparisons. The backward pass requires a matrix multiplication with the derivative of Maxpool (which is a unit vector with 0's everywhere except at the location of the argmax). For optimization, we compute this while computing the Maxpool in the forward pass. Since pooling layers do not introduce any parameters, there is no parameter update required for this layer.

$$a_{x,y,d,b}^l = \left(\max_{p,q} a_{xS+p,yS+q,d',b'}^{l-1} \right) \cdot \epsilon_{dd'} \epsilon_{bb'} \quad (16a)$$

$$\delta_{\alpha,\beta,r,b}^{l-1} = \left(\delta_{x,y,r,b}^l \otimes f_{xS+p,yS+q,r',b'} \right) \cdot \quad (16b)$$

$$\epsilon_{rr'} \epsilon_{bb'} \epsilon_{\alpha(xS+p)} \epsilon_{\beta(yS+q)} \quad (16c)$$

Here, f denotes the derivative of the Maxpool function. Equation 16a governs the forward pass and equation 16c governs the back-prop.

B.4 Normalization Layer

Normalization is typically applied to the output of the first few layers for improved performance on two fronts – stability

and efficiency of training. Activations are normalized across a batch by subtracting the mean and dividing by the standard deviation. Finally, these normalized inputs are then scaled using two learnable parameters γ, β .

$$\mu_b = \sum_{\alpha, \beta, r} a_{\alpha, \beta, r, b}^{l-1} \quad (17a)$$

$$\sigma_b^2 = \frac{1}{m} \sum_{\alpha, \beta, r} (a_{\alpha, \beta, r, b}^{l-1} - \mu_b)^2 \quad (17b)$$

$$z_{\alpha, \beta, r, b}^{l-1} = \frac{(a_{\alpha, \beta, r, b}^{l-1} - \mu_b)}{\sqrt{\sigma_b^2 + \epsilon}} \quad (17c)$$

$$a_{\alpha, \beta, r, b}^l = \gamma z_{\alpha, \beta, r, b}^{l-1} + \beta \quad (17d)$$

where m is the size of each batch. We set $\epsilon = 2^{-10}$. Equations 17a-17d form the forward pass of the batch norm layer. The back-prop and update parameters are simply matrix multiplications and are omitted due to space constraints.

B.5 ReLU Activation

Rectified Linear Unit (ReLU) defined as $(x) = \max(0, x)$ is one of the most popular activation functions used in deep learning. It is applied to the output of most layers and simply applies the ReLU function to each input. Hence, the input and output both are matrices in $\mathbb{R}^{s_{in} \times B}$. Since the output is a fixed function of the inputs, there are no learnable parameters in this layer. The forward pass involves computing the ReLU function on each input whereas the backward pass involves a matrix multiplication with the derivative of ReLU function (which is 0 if the input is negative and 1 otherwise). There is not parameter update.

We use Stochastic Gradient Descent (SGD) to iteratively train the network to learn the right set of parameter values. We use the cross entropy loss function for training given by:

$$C = -\frac{1}{n} \sum_b \sum_j (y_j \ln a_{j,b}^L + (1 - y_j) \ln(1 - a_{j,b}^L)) \quad (18)$$

where n is the batch size. These above 5 layers, can be used to implement a large fraction of the neural networks used in deep learning and specifically in computer vision.

C Datasets

We select 3 datasets popularly used for training image classification models — MNIST [16], CIFAR-10 [17], and Tiny ImageNet [18]. We describe each of these briefly below:

- (A) **MNIST [16]:** MNIST is a collection of handwritten digits dataset. It consists of 60,000 images in the training set and 10,000 in the test set. Each image is a 28×28 pixel image of a handwritten digit along with

a label between 0 and 9. We evaluate Network-A, B, C, and the LeNet network on this dataset in both the semi-honest and maliciously secure variants.

- (B) **CIFAR-10 [17]:** CIFAR-10 consists of 60,000 images (50,000 training and 10,000 test images) of 10 different classes (such as airplanes, dogs, horses etc.). There are 6,000 images of each class with each image consisting of a colored 32×32 image. We perform private training and inference of AlexNet and VGG16 on this dataset.

- (C) **Tiny ImageNet [18]:** Tiny ImageNet dataset consists of 100,000 training samples and 10,000 test samples with 200 different classes [18]. Each sample is cropped to a size of $64 \times 64 \times 3$. We perform private training and inference of AlexNet and VGG16 on this dataset.

D Network Architectures

Layer	Input Size	Description	Output
Fully Connected Layer	28×28	Fully connected layer	128
ReLU Activation	128	ReLU(\cdot) on each input	128
Fully Connected Layer	128	Fully connected layer	128
ReLU Activation	128	ReLU(\cdot) on each input	128
Fully Connected Layer	128	Fully connected layer	10
ReLU Activation	10	ReLU(\cdot) on each input	10

Figure 3: Neural Network architecture from SecureML [6] for training over MNIST dataset.

Layer	Input Size	Description	Output
Convolution	$32 \times 32 \times 3$	Window size 3×3 , Stride (1, 1), Padding (1, 1), output channels 64	$32 \times 32 \times 64$
ReLU Activation	$32 \times 32 \times 64$	ReLU(\cdot) on each input	$32 \times 32 \times 64$
Convolution	$32 \times 32 \times 64$	Window size 3×3 , Stride (1, 1), Padding (1, 1), output channels 64	$32 \times 32 \times 64$
ReLU Activation	$32 \times 32 \times 64$	ReLU(\cdot) on each input	$32 \times 32 \times 64$
Max Pooling	$32 \times 32 \times 64$	Window size 2×2 , Stride (2, 2)	$16 \times 16 \times 64$
Convolution	$16 \times 16 \times 64$	Window size 3×3 , Stride (1, 1), Padding (1, 1), output channels 128	$16 \times 16 \times 128$
ReLU Activation	$16 \times 16 \times 128$	ReLU(\cdot) on each input	$16 \times 16 \times 128$
Convolution	$16 \times 16 \times 128$	Window size 3×3 , Stride (1, 1), Padding (1, 1), output channels 128	$16 \times 16 \times 128$
ReLU Activation	$16 \times 16 \times 128$	ReLU(\cdot) on each input	$16 \times 16 \times 128$
Max Pooling	$16 \times 16 \times 128$	Window size 2×2 , Stride (2, 2)	$8 \times 8 \times 128$
Convolution	$8 \times 8 \times 128$	Window size 3×3 , Stride (1, 1), Padding (1, 1), output channels 256	$8 \times 8 \times 256$
ReLU Activation	$8 \times 8 \times 256$	ReLU(\cdot) on each input	$8 \times 8 \times 256$
Convolution	$8 \times 8 \times 256$	Window size 3×3 , Stride (1, 1), Padding (1, 1), output channels 256	$8 \times 8 \times 256$
ReLU Activation	$8 \times 8 \times 256$	ReLU(\cdot) on each input	$8 \times 8 \times 256$
Convolution	$8 \times 8 \times 256$	Window size 3×3 , Stride (1, 1), Padding (1, 1), output channels 256	$8 \times 8 \times 256$
ReLU Activation	$8 \times 8 \times 256$	ReLU(\cdot) on each input	$8 \times 8 \times 256$
Max Pooling	$8 \times 8 \times 256$	Window size 2×2 , Stride (2, 2)	$4 \times 4 \times 256$
Convolution	$4 \times 4 \times 256$	Window size 3×3 , Stride (1, 1), Padding (1, 1), output channels 512	$4 \times 4 \times 512$
ReLU Activation	$4 \times 4 \times 512$	ReLU(\cdot) on each input	$4 \times 4 \times 512$
Convolution	$4 \times 4 \times 512$	Window size 3×3 , Stride (1, 1), Padding (1, 1), output channels 512	$4 \times 4 \times 512$
ReLU Activation	$4 \times 4 \times 512$	ReLU(\cdot) on each input	$4 \times 4 \times 512$
Convolution	$4 \times 4 \times 512$	Window size 3×3 , Stride (1, 1), Padding (1, 1), output channels 512	$4 \times 4 \times 512$
ReLU Activation	$4 \times 4 \times 512$	ReLU(\cdot) on each input	$4 \times 4 \times 512$
Max Pooling	$4 \times 4 \times 512$	Window size 2×2 , Stride (2, 2)	$2 \times 2 \times 512$
Convolution	$2 \times 2 \times 512$	Window size 3×3 , Stride (1, 1), Padding (1, 1), output channels 512	$2 \times 2 \times 512$
ReLU Activation	$2 \times 2 \times 512$	ReLU(\cdot) on each input	$2 \times 2 \times 512$
Convolution	$2 \times 2 \times 512$	Window size 3×3 , Stride (1, 1), Padding (1, 1), output channels 512	$2 \times 2 \times 512$
ReLU Activation	$2 \times 2 \times 512$	ReLU(\cdot) on each input	$2 \times 2 \times 512$
Convolution	$2 \times 2 \times 512$	Window size 3×3 , Stride (1, 1), Padding (1, 1), output channels 512	$2 \times 2 \times 512$
ReLU Activation	$2 \times 2 \times 512$	ReLU(\cdot) on each input	$2 \times 2 \times 512$
Max Pooling	$2 \times 2 \times 512$	Window size 2×2 , Stride (2, 2)	$1 \times 1 \times 512$
Fully Connected Layer	512	Fully connected layer	4096
ReLU Activation	4096	ReLU(\cdot) on each input	4096
Fully Connected Layer	4096	Fully connected layer	4096
ReLU Activation	4096	ReLU(\cdot) on each input	4096
Fully Connected Layer	4096	Fully connected layer	1000
ReLU Activation	1000	ReLU(\cdot) on each input	1000

Figure 4: VGG16 network architecture [14] for training over CIFAR-10 dataset.

Layer	Input Size	Description	Output
Convolution	$28 \times 28 \times 1$	Window size 5×5 , Stride (1, 1), Padding (0, 0), output channels 16	$24 \times 24 \times 16$
ReLU Activation	$24 \times 24 \times 16$	ReLU(\cdot) on each input	$24 \times 24 \times 16$
Max Pooling	$24 \times 24 \times 16$	Window size 2×2 , Stride (2, 2)	$12 \times 12 \times 16$
Convolution	$12 \times 12 \times 16$	Window size 5×5 , Stride (1, 1), Padding (0, 0), output channels 16	$8 \times 8 \times 16$
ReLU Activation	$8 \times 8 \times 16$	ReLU(\cdot) on each input	$8 \times 8 \times 16$
Max Pooling	$8 \times 8 \times 16$	Window size 2×2 , Stride (2, 2)	$4 \times 4 \times 16$
Fully Connected Layer	256	Fully connected layer	100
ReLU Activation	100	ReLU(\cdot) on each input	100
Fully Connected Layer	100	Fully connected layer	10
ReLU Activation	10	ReLU(\cdot) on each input	10

Figure 5: Neural network architecture used in MiniONN [19] for training over MNIST dataset.

Layer	Input Size	Description	Output
Convolution	$32 \times 32 \times 3$	Window size 11×11 , Stride (4, 4), Padding (9, 9), output channels 96	$11 \times 11 \times 96$
ReLU Activation	$11 \times 11 \times 96$	ReLU(\cdot) on each input	$11 \times 11 \times 96$
Max Pooling	$11 \times 11 \times 96$	Window size 3×3 , Stride (2, 2)	$5 \times 5 \times 96$
Batch Normalization	$5 \times 5 \times 96$	Normalization and linear scaling using learnable parameters γ, β	$5 \times 5 \times 96$
Convolution	$5 \times 5 \times 96$	Window size 5×5 , Stride (1, 1), Padding (1, 1), output channels 256	$3 \times 3 \times 256$
ReLU Activation	$3 \times 3 \times 256$	ReLU(\cdot) on each input	$3 \times 3 \times 256$
Max Pooling	$3 \times 3 \times 256$	Window size 3×3 , Stride (2, 2)	$1 \times 1 \times 256$
Batch Normalization	$1 \times 1 \times 256$	Normalization and linear scaling using learnable parameters γ, β	$1 \times 1 \times 256$
Convolution	$1 \times 1 \times 256$	Window size 3×3 , Stride (1, 1), Padding (1, 1), output channels 384	$1 \times 1 \times 384$
ReLU Activation	$1 \times 1 \times 384$	ReLU(\cdot) on each input	$1 \times 1 \times 384$
Convolution	$1 \times 1 \times 384$	Window size 3×3 , Stride (1, 1), Padding (1, 1), output channels 384	$1 \times 1 \times 384$
ReLU Activation	$1 \times 1 \times 384$	ReLU(\cdot) on each input	$1 \times 1 \times 384$
Convolution	$1 \times 1 \times 384$	Window size 3×3 , Stride (1, 1), Padding (1, 1), output channels 256	$1 \times 1 \times 256$
ReLU Activation	$1 \times 1 \times 256$	ReLU(\cdot) on each input	$1 \times 1 \times 256$
Fully Connected Layer	256	Fully connected layer	256
ReLU Activation	256	ReLU(\cdot) on each input	256
Fully Connected Layer	256	Fully connected layer	256
ReLU Activation	256	ReLU(\cdot) on each input	256
Fully Connected Layer	256	Fully connected layer	10
ReLU Activation	10	ReLU(\cdot) on each input	10

Figure 6: AlexNet network architecture [15] for training over CIFAR-10 dataset.

Layer	Input Size	Description	Output
Convolution	$28 \times 28 \times 1$	Window size 5×5 , Stride (1, 1), Padding (0, 0), output channels 20	$24 \times 24 \times 20$
ReLU Activation	$24 \times 24 \times 20$	ReLU(\cdot) on each input	$24 \times 24 \times 20$
Max Pooling	$24 \times 24 \times 20$	Window size 2×2 , Stride (2, 2)	$12 \times 12 \times 20$
Convolution	$12 \times 12 \times 20$	Window size 5×5 , Stride (1, 1), Padding (0, 0), output channels 50	$8 \times 8 \times 50$
ReLU Activation	$8 \times 8 \times 50$	ReLU(\cdot) on each input	$8 \times 8 \times 50$
Max Pooling	$8 \times 8 \times 50$	Window size 2×2 , Stride (2, 2)	$4 \times 4 \times 50$
Fully Connected Layer	800	Fully connected layer	500
ReLU Activation	500	ReLU(\cdot) on each input	500
Fully Connected Layer	500	Fully connected layer	10
ReLU Activation	10	ReLU(\cdot) on each input	10

Figure 7: LeNet network architecture [33] for training over MNIST dataset.

Layer	Input Size	Description	Output
Convolution	$28 \times 28 \times 1$	Window size 2×2 , Stride (2, 2), Padding (0, 0), output channels 5	$14 \times 14 \times 5$
ReLU Activation	$14 \times 14 \times 5$	ReLU(\cdot) on each input	$14 \times 14 \times 5$
Fully Connected Layer	980	Fully connected layer	100
ReLU Activation	100	ReLU(\cdot) on each input	100
Fully Connected Layer	100	Fully connected layer	10
ReLU Activation	10	ReLU(\cdot) on each input	10

Figure 8: Neural network architecture used in Chameleon [11] for training over MNIST dataset.

E Functionality Descriptions

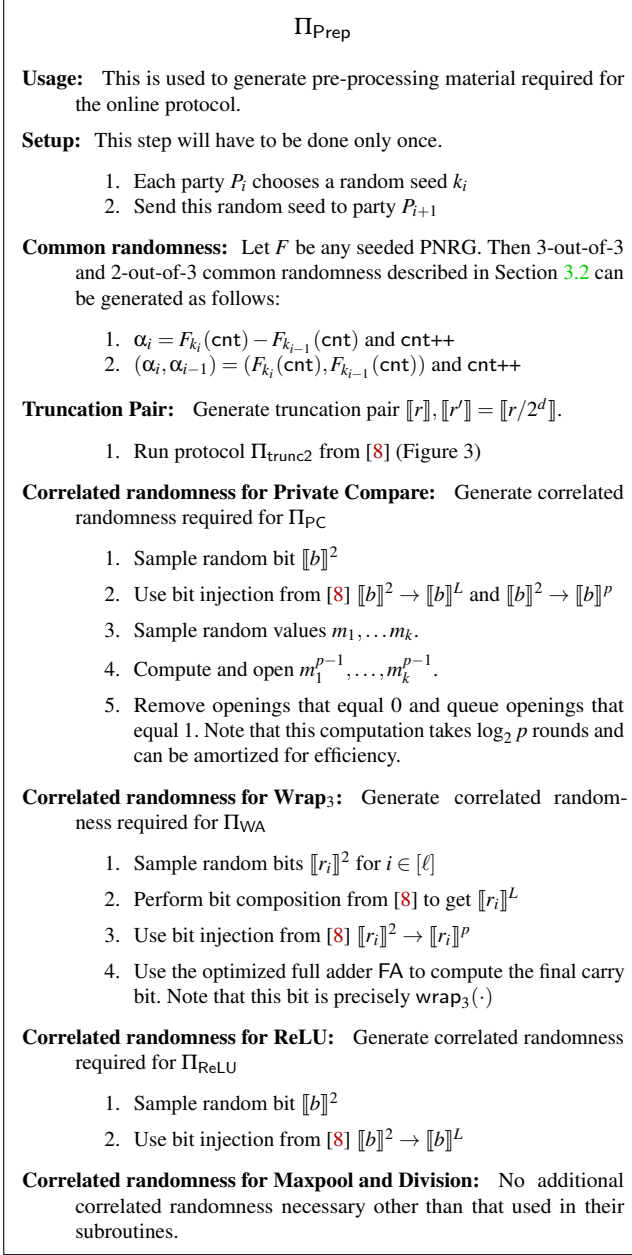


Figure 1: Protocols for generating various pre-processing material

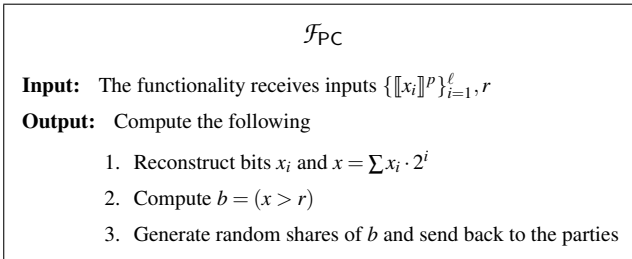


Figure 9: Ideal functionality for Π_{PC}

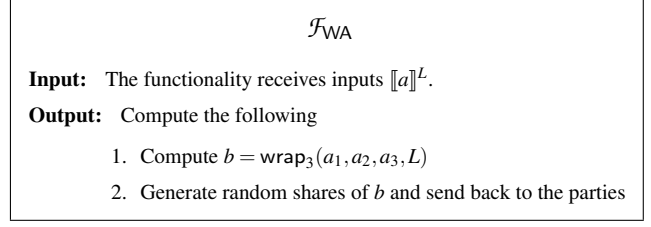


Figure 10: Ideal functionality for Π_{WA}

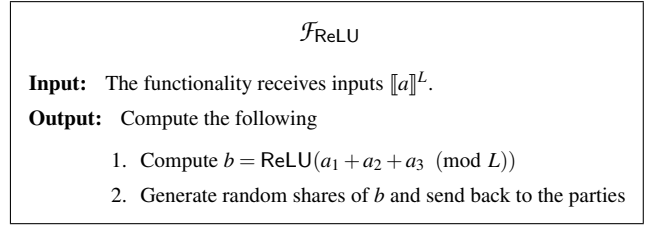


Figure 11: Ideal functionality for Π_{ReLU}

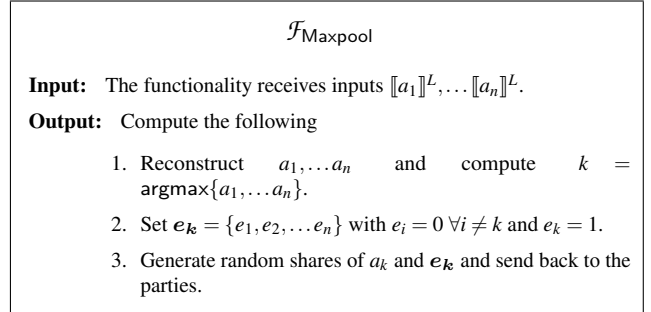


Figure 12: Ideal functionality for Π_{Maxpool}

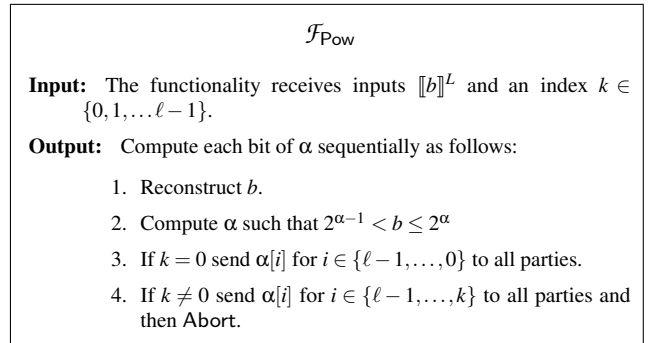


Figure 13: Functionality for Π_{Pow}

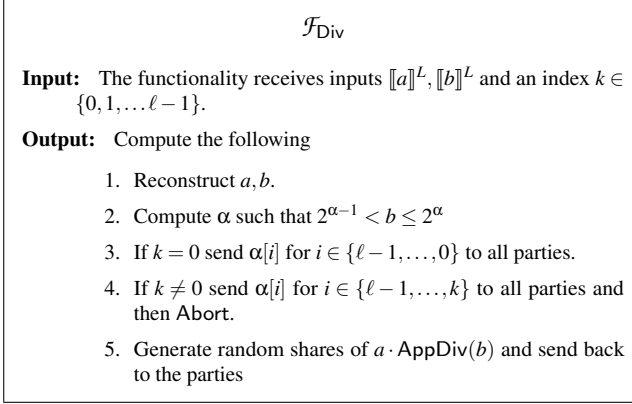


Figure 14: Ideal functionality for Π_{Div}

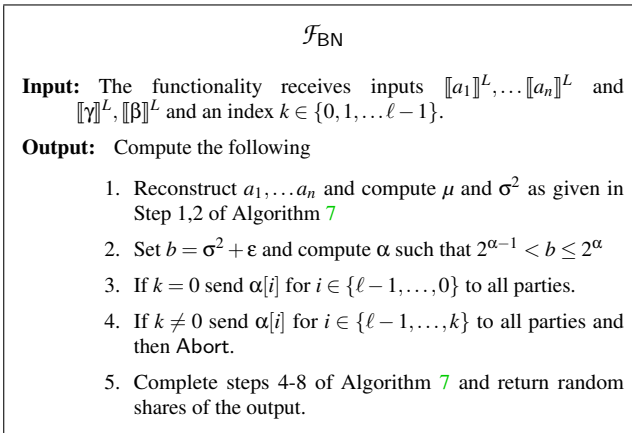


Figure 15: Ideal functionality for Π_{BN}